EFFECT OF REINFORCEMENT CORROSION ON STATIC AND DYNAMIC BEHAVIOUR OF RC BEAMS

A Dissertation Submitted

In Partial Fulfillment of the Requirements

For the degree of

MASTER OF ENGINEERING

IN

STRUCTURAL ENGINEERING

Submitted By

ANMOL RATTAN

Roll No. 801322005

Under the Supervision of

Dr Naveen Kwatra
Professor and Head
Civil Engineering Department
Thapar University, Patiala

Dr Shruti Sharma
Associate Professor
Civil Engineering Department
Thapar University, Patiala

2015

DEPARTMENT OF CIVIL ENGINEERING,

THAPAR UNIVERSITY,

PATIALA-147004, INDIA

DECLARATION

The author hereby declare that this dissertation entitled *"EFFECT OF REINFORCEME CORROSION ON STATIC AND DYNAMIC BEHAVIOUR OF RC BEAMS "* in whole or part has n been used to obtain any degree in this, or any other, institute, except where references have been given text, it is entirely the author's own work. The author confirm that the library may lend or copy this up request for academic purposes.

Anmol Ratta

ANMOL RATTA
8013220

CERTIFICATE

It is certified that the dissertation report entitled *"EFFECT OF REINFORCEMENT CORROSION O STATIC AND DYNAMIC BEHAVIOUR OF RC BEAMS "* which is being submitted here with b **Anmol Rattan,** in partial fulfillment for the award of degree in masters of **Civil Engineering (Structures** at **Thapar University, Patiala** is an authentic record of student's own work carried out under m supervision and guidance. The matter presented in the dissertation has reached the standards fulfilling th requirements of the regulation for the award of said degree.

21/7/15

Dr .NAVEEN KWATRA
Professor and Head
Department of Civil Engineering
Thapar University,Patiala

Shruti Sharma

Dr. SHRUTI SHARMA
Associate Professor
Department of Civil Engineering
Thapar University,Patiala

COUNTERSIGNED BY

31/7/15

Dr.NAVEEN KWATRA
Professor and Head
Department of Civil Engineering
Thapar University,Patiala

Dr. S. S.BHATIA
Dean , Academic Affairs
Department of Civil Engineering
Thapar University,Patiala

ACKNOWLEDGEMENT

I would like to thank God for not letting me down at the time of crisis and showing me the silver lining in the dark clouds. I wish to express my deep gratitude to Dr. Naveen Kwatra, Professor and Head, Civil Engineering Department, Thapar University Patiala and Dr. Shruti Sharma, Associate Professor , Civil Engineering Department Thapar University Patiala for providing their uncanny guidance, support and for their patient listening of my ideas and also suggesting new ways for implementing my ideas and for the motivation and inspiration that triggered me throughout my work.

I would also thank to my parents and brother for their constant encouragement during my entire work.

I would also like to thank Mr Ram Simran , Lab Attendantant, Thapar University, Patiala for his support in my entire work.

I m also like to offer my thanks to all the staff members and my co-students who were always there at the need of the hour and provided with all the help and facilities, which I required for the completion of the project report.

Anmol Rattan

Anmol Rattan

801322005

ABSTRACT

Reinforced concrete structures have not been immune to the ravages of corrosion despite the protection that concrete provides to embedded steel. Since steel corrosion remains unnoticed inside the concrete, it further accelerates and can cause loss of life and property. This report discusses the effects of deterioration caused to reinforced beams due to corrosion at different levels and analyses the same by static and dynamic procedure. Four RC beams (127 x 227 x 4100) mm were cast one was kept as control beam and rest three of which were corroded to different levels i.e. (7days, 15days, 24days) by impressed current technique, while one remain as control beam . All four beams were subjected to vibration based health monitoring at the end of their respective corrosion period. This was done to investigate the effect of corrosion on dynamic properties of beams with increasing corrosion.Vibration characteristices of beams showed decrease in vibration amplitude and frequency of beam with increasing level of corrosion. After dynamic analysis ,each beam was tested under static four-point loading and corresponding loads and deflections were recorded. The static load deflection characteristices of beams corroded to different level shows decrease in load carrying capacity,deflection capacity with the increase in age of corrosion. Most importantly it was noticed that as corrosion increased the failure mode of beams shifts from predictable ductile failure to brittle failure.

CONTENTS

DECLARATION i

CERTIFICATE i

ACKNOWLEDGEMENT ii

ABSTRACT iii

LIST OF FIGURES vii

LIST OF FIGURES x

CHAPTER- 1 INTRODUCTION 1-21

1.1 Background 1

1.2Corrosion in RC structures 2

1.2.1 Corrosion Mechanism 3

1.2.3 Effect of Corrosion on Structural Capacity 6

1.2.4 Effect on Steel 8

1.2.5 Effect on Concrete 8

1.2.6 Electrochemical Methods to measure Corrosion 9

1.2.7 Effectiveness of Impressed Current Technique to Stimulate Corrosion of Steel Reinforcement in Concrete 10

1.3 Structural health monitoring (SHM) 11

1.3.2 Techniques for SHM 13

1.3.2.1 Local Techniques 13

1.3.2.2 Methods for Local Techniques 14

1.3.2.3 Global Technique 18

1.4 Global Analysis Using Vibration Measurement 19

1.5 Objectives and Scope of Work 21

1.6 Closing Remarks 21

CHAPTER -2 LITERATURE SURVEY 22-33

2.1 Literature review on effect of corrosion on RC structures 22

2.2 Literature survey on vibration monitoring 29

2.3 Closing Remarks 33

CHAPTER-3 EXPERIMENTAL INVESTIGATION 34-44

3.1 Test matrix and program 34

3.2 Materials 34

3.3 Design mix proportions of concrete 38

3.4 RCC Beam Design 38

3.5 Casting of Composite Beams 39

3.6 Inducing Corrosion in RC Beam 40

3.7 Study of Load-Deflection Characteristic 41

3.8 Vibration monitoring 42

3.8.1 Equipments used in vibration monitoring 43

3.9 Closing Remarks 44

CHAPTER-4 RESULTS AND DISCUSSIONS 45-66

4.1 Visual Inspection 45

4.1.1 Beam corroded to 7 days(C-7) 45

4.1.2 Beam corroded to 15 days (C-15) 47

4.1.3 Beam corroded to 24day(C-24) 49

4.2 Load Deflection behaviour of RC beam 51

4.2.1Control Beam (C-0) 51

4.2.2 Beams corroded to 7 days (C-7) 53

4.2.3 Beams Corroded to 15-Days (C-15) 55

4.2.4Beams corroded to 24 days (C-24) 57

4.3 Comparison of Load Deflection characteristices of all beams 57

4.4 Vibration Characteristics of beams at Center 59

4.4.1 Control beam (C-0) 61

4.4.2 Beam corroded to 7 days (C-7) 61

4.4.3 Beam corroded to 15 days(C-15) 62

4.4.4 Beam corroded to 24 days(C-24) 62
4.5 Variation of frequency with level of corrosion 63
4.6 Variation of FRF amplitude with level of corrosion 64
4.7 Calculation of Damage index 65
4.8 Closing Remark 66
CHAPTER -5 CONCLUSIONS **67-68**
5.1 VISUAL INSPECTION 67
5.2 STATIC ANALYSIS 67
5.3 DYNAMIC ANALYSIS 68
REFERENCES **69-72**

LIST OF FIGURES

FIGURE NO.	HEADINGS	PAGE NO.
Fig 1.1	Corrosion in RC structures	3
Fig 1.2	(a) the anodic and cathodic re actions (B roomfield,1997) (b) Anodic and Cathodic re actions on s teel (B roomfie ld, 1997)	4
Fig 1.3	Corrosion Cycle in Reinforced Concrete (Andrade .et.al., 1996)	8
Fig 1.4	Circuit for electrical resistance measurements (Song and Saraswathy,2007)	15
Fig 1.5	Cover meter (Song and Saraswathy, 2007	16
Fig 1.6	Schematic representation of surface potential (SP) measurement Song and Saraswathy,2007	16
Fig 1.7	Linear polarization resistance measurement Song and Saraswathy 2007	17
Fig 1.8	Set-up for galvanostatic pulse technique Song and Saraswathy,2007	18
Fig 2.1	General view for accelerated corrosion (Maaddawy et al., 2003	22
Fig 2.2	Load Deflection Behavior for all beam specimens Joyce 2008	24
Fig 2.3	Reinforcement configuration for test beams and accelerated corrosion Setup,Malumbela et al 2009	24
Fig 2.4	Variation in longitudinal strains on the corroded region with time Malumbela et al., 2009	25
Fig 2.5	Variation in depth of the neutral axis on the corroded region with time, Malumbela et al.,2009	26
Fig 2.6	Variation in curvature on the corroded region with time. Malumbela et al., 2009	26
Fig 2.7	Variation in moment of inertia on the corroded region with time Malumbela et al.,2009	27
Fig 2.8	Static Stiffness of Rigid beam Constrained by two Discrete Springs Waters	30

Fig 2.9	(a)-(d) Relation of Frequency to Temperature Hang Hao et al. (2006)	32
Fig 3.1	Specimen details	39
Fig 3.2	Beam mould with reinforcement cage	39
Fig 3.3	Beam after casting	39
Fig 3.4	DC Regulated D ual Powe r S upply Source	40
Fig 3.5	Stainless steel wire mesh wrapped around central 1.5 m part of concrete beam served as cathode	40
Fig 3.6	Hydraulic operated jack	41
Fig 3.7	Data aquisition sytem	41
Fig 3.8	LVDT	42
Fig 3.9	Accelerometer placed below at center postion of beam	42
Fig 3.10	Various arrangements in software	43
Fig 4.1	Bottom face of C-7	46
Fig 4.2	Right side of front face of C-7	46
Fig 4.3	Red brownish products observed along the side	46
Fig 4.4	Bottom face of C-15	47
Fig 4.5	Flexural crack at centre of C-15	47
Fig 4.6	Longitudnal and transverse cracks at right face of C-15	48
Fig 4.7	Cracks on left side of C-15	48
Fig 4.8	Spalling of concrete in C-15	49
Fig 4.9	Removal of concrete cover of C-15	49
Fig 4.10	Long vertical crack at centre of beam results in breaking of beam	50
Fig 4.11	Dark reddish brown corrosion products	50
Fig 4.12	Long horizontal cracks at the bottom side of front face	51
Fig 4.13	Flexure Cracks on side face of C-0 beam	52
Fig 4.14	Load deflection curve of control beam C-0 at L/2	52
Fig 4.15	Load deflection curve of control beam C-0 at L/4	53
Fig 4.16	Side face of C-7 Beam before load	53
Fig 4.17	C-7 beam showing huge crack at centre after failure	54
Fig 4.18	Load deflection of corroded beam after 7days at L/2	55

Fig 4.19	Load deflection curve for corroded beam after 7 days at L/4 span	55
Fig 4.20	Side face of C-15 Beam before loading	56
Fig 4.21	C-15 beam showing large vertical crack near the centre of beam	56
Fig 4.22	Load deflection characteristics of C-15 at L/2	57
Fig 4.23	Load deflection characteristics of C-15 at L/4	57
Fig 4.24	Bar chart showing stiffness loss with corosion in beams	58
Fig 4.25	FRF record of control beam	61
Fig 4.26	FRF record of corroded beam to 7 days	61
Fig 4.27	FRF record of corroded beam to 15 days	62
Fig 4.28	FRF record of corroded beam to 24 days	62
Fig 4.29	Bar chart showing relation between level of corrosion with frequency	63
Fig 4.30	Bar chart showing relation between level of corrosion with FRF amplitude	64
Fig 4.31	Graph showing relation between damage index and FRF magnitude	65

LIST OF TABLES

TABLE NO.	HEADINGS	PAGE NO.
Table 1.1	Parameters affecting the corrosion process (Webster, 2000)	5
Table 1.2	Summary of Some Previous Accelerated Corrosion Tests	11
Table 2.1	Decrease in Flexural Stiffness Acosta et. al., (2004)	28
Table 3.1	Physical Properties of Cement used	35
Table 3.2	Sieve analysis of fine aggregate	35
Table 3.3	Properties of fine aggregates	36
Table 3.4	Sieve analysis of 10mm aggregates	36
Table 3.5	Sieve analysis of 20 mm aggregates	37
Table 3.6	Physical Properties of Coarse Aggregates	37
Table 3.7	Physical Properties of Steel Bars	38
Table 4.1	Load deflection characteristices of control beam	52
Table 4.2	Beam corroded to 7 days	54
Table 4.3	Beam corroded to 15 days	56
Table 4.4	Stiffness loss	58
Table 4.5	Relation of level of corrosion with frequency	63
Table 4.6	Relation of level of corrosion with FRF amplitude	64
Table 4.7	Variation of damage index with FRF magnitude and frequenccy	65

CHAPTER-1
INTRODUCTION

1.1 Background

It is often the case that a large amount of reinforced concrete (RC) structures such as highway or railway bridges are damaged because of the corrosion of the steel rebar. It has been a hotspot in the structural rehabilitation to conduct degradation evaluation of the mechanical behavior of the existing reinforced concrete structures by corrosion. The primary effects can be roughly categorized into: (1) the reduction of the effective diameter of reinforcement bars; (2) the loss of bond between steels; (3) the concrete and the micro cracking of the concrete due to the expansion of the bars by the rust products as a consequence of electrochemical processes (Wang .et.al.,2015).

The major research papers on reinforcement corrosion are focusing on mechanism of corrosion, assessment of strength, load carrying capacity ,deflections and stiffness affected by reinforcement corrosion.As we induce corrosion in the structure it directly affects its static properties as well as flexural capacity.If we increase the level of corrosion in RC structures,it results in weakening bond of concrete and steel leads to decreased strength of structure.

Reinforcement corrosion also effects the dynamic behaviour of structures i.e natural frequency , damping, vibration amplitude.However, natural frequency is a good overview of the global structural condition. It was found to be a good indicator of damage.Dynamic properties of structure can change whenever damping, mass or stiffness is changed.

Generally, structural vibrations are damped forced vibrations. This means that the applied forcing disturbance will produce a magnified vibration structures. The change in stiffness, mass or damping would appear to be the dominant consequence of deterioration. Vibration monitoring involves the relationship between applied force and the resulting vibration. Techniques of vibration monitoring are well developed and for many structures the use of vibration monitoring techniques can be recommended without restriction . Vibration of

a structural element, frequency ranges, and vibration amplitude depend on many factors such as material, supports, cross-section area. (Rao, 2000)

1.2 Corrosion in RC structures

Reinforced concrete (RC) has been developed and applied extensively in the twentieth century and it continues to be used in this century as well. It combines the good compressive strength of concrete with the tensile strength of steel and has proven to be successful in terms of both structural performance and durability. One major flaw, namely its susceptibility to environmental attack can severely reduce the strength and life of these structures. In humid conditions,atmospheric pollutants percolate through the concrete cover and cause corrosion of steel reinforcements. The resulting corrosion products occupy volumes several times that of the steel. The increased volume induces tensile stresses in the concrete that result in cracking, delamination and spalling. As a result, the reinforcements get exposed to direct environmental attack and the corrosion is accelerated. Along with unpleasant appearance **(Fig 1.1)** it weakens the concrete structure to a high degree. Moreover, bond between the steel and the concrete is reduced.Pitting corrosion may also reduce the ductility of the steel bar by introducing notches on the surface of the steel bars that leads to a premature necking (Andrade et al,1993).

A large proportion of damage is caused due to insufficient planning and incorrect assessment of the environmental attack such as carbonation and chloride exposure. Corrosion affected structures are highly susceptible to catastrophic collapse. Unlike other devices and facilities that are renewed periodically with newer ones human endeavor has been to maintain centuries old structures. As a result,structural engineers deal with RC structures of age varying more than hundred years. They are also subjected to a wide range of environmental load regimes. Typically, an RC structure that is subjected to heavy environmental loading requires major restoration work within fifteen years of its construction.

(1) Corrosion in columns

(2) Corrosion in beams

(3) Corrosion in slabs

Fig 1.1 Corrosion in RC structures(Andrade et al,1993)

1.2.1 Corrosion Mechanism

Corrosion is the process of the transformation of a metal to its "native" form, which is the natural ore state, often as oxides, chlorides or sulphates. This transformation occurs because the compounds such as the oxides "involve" less energy than pure metals, and hence they are more stable thermodynamically. The corrosion process does not take place directly but rather as a series of electrochemical reactions with the passage of an electric current. Corrosion also depends on the type and nature of the metal, the immediate environment, temperature and other related factors. The corrosion may be defined as the destructive attack of a metal by chemical or electrochemical reaction with its environment. Steel in concrete is normally immune from corrosion because of the high alkalinity of the concrete,the pH of the pore water can be greater than 12.5, which protects the embedded steel against corrosion. This alkalinity of concrete causes passivation of the embedded reinforcing bars.

A microscopic oxide layer, which is the “passive” film, forms on the steel surface due to the high pH, which prevents the dissolution of iron. Furthermore, the concretes made using low water-cement ratios and good curing practices have a low permeability, which minimizes the penetration of the corrosion inducing ingredients. In addition, low permeability is believed to increase the electrical resistivity of the concrete to some degree which helps in reducing the rate of corrosion by retarding the flow of electrical currents within the concrete that accompany the electrochemical corrosion. Consequently, corrosion of the embedded steel requires the breakdown of its passivity.Once the passive layer on the reinforcing steel has been disrupted and corrosion is activated, the chemical reactions are similar whether the corrosion was initiated by chloride attack or by carbonation. The principal cause of steel corrosion is the presence of chlorides during the preparation of the concrete. In several places close to shore, even sea sand is used as an aggregate. Some chemical admixtures, as accelerators, can contain high percentage of chlorides. De- icing salts used during winter time can introduce chlorides to the reinforced steel. The corrosion process caused by chlorides in steel is shown below in **Fig 1.2**(Broom field, 1997)

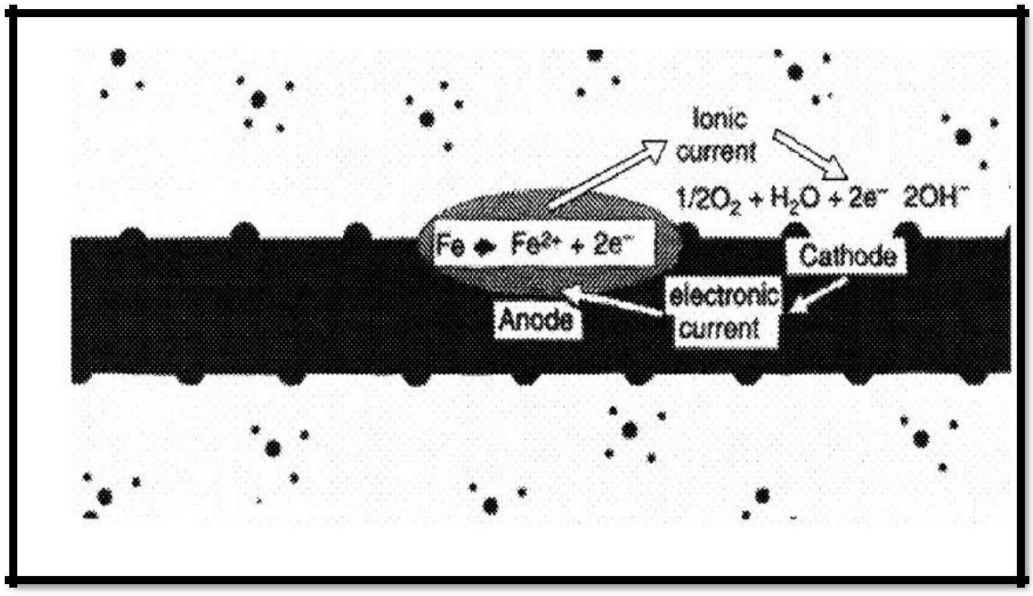

Fig 1.2 (a) The anodic and cathodic re actions (B room field, 1997)

Ferrous hydroxide forms as the 2Fe++ ions at the anode combine with the hydroxide ions flowing from the cathode. In the presence of oxygen and moisture, the ferrous hydroxide converts to ferric oxide i.e. rust. The quantity of iron that reacts (rusts) is proportional to the

corrosion current and time in accordance with Faraday's law. This law is used in many of the tests described in the following sections

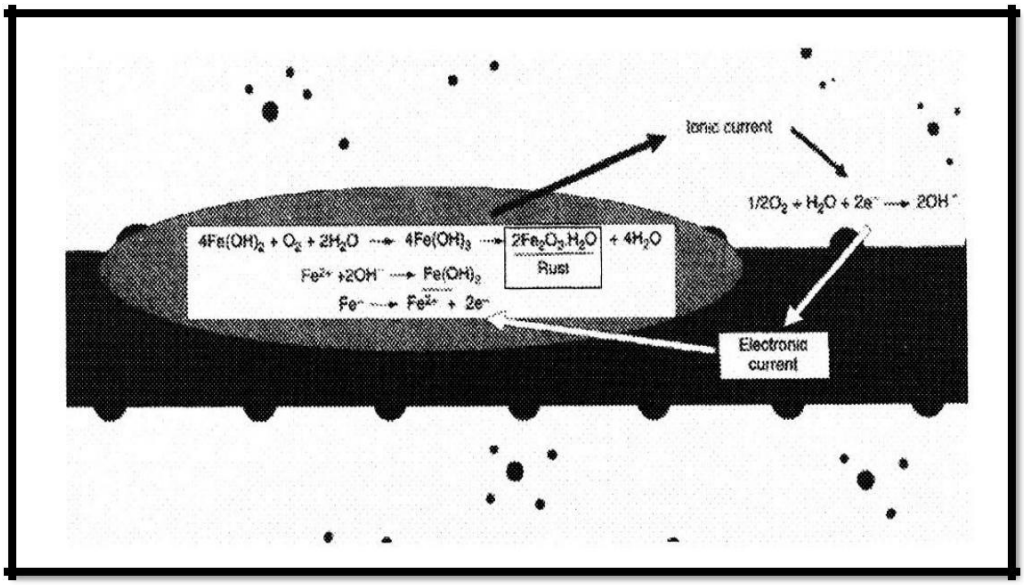

Fig 1.2 (b) Anodic and Cathodic re actions on steel (B room field, 1997)

When unhydrated, ferric oxide is dense and has a volume of around twice that of the steel it replaces. When it becomes hydrated (takes in water) it swells and becomes porous. This swelling can lead to a volume increase of between two to four- fold at the steel-concrete interface.This gives the flaky red/brown rust on the reinforcing bar and can cause cracking (and spalling) of the cover concrete. Some of the rust will be accommodated in the concrete pore structure adjacent to the corroding bar. Corrosion is the loss of iron at the anode, whilst rust is the product formed at the cathode.(Webster,2000) The effects of various parameters on the corrosion process are summarized in Table 1.1

Table 1.1 Parameters affecting the corrosion process (Webster, 2000)

Parameters affecting the corrosion process	
Parameter	*Effect*
Moisture	Moisture is required initially for the cathodic reaction and then for rust formation at the anode. Without sufficient moisture, the rate of corrosion will be negligible.
Oxygen	Oxygen is required initially for the cathodic reaction and then for rust formation at the anode. It is possible that chloride-induced corrosion will be controlled by oxygen availability as chlorides typically enter with moisture. With low levels of oxygen, the rate of corrosion will be negligible.
Resistivity	The higher the resistivity, the lower the corrosion current will be. Resistivity increases with temperature, and decreases with increasing moisture content (RH).

1.2.3 Effect of Corrosion on Structural Capacity

There are three broad types of corrosion experienced by reinforcing bars namely, **Pitting**, **General** and **Macro-cell** corrosion. The factors governing these types of corrosion are discussed below.

Pitting corrosion

Pitting corrosion is most likely to occur in concrete with good conductivity, a high content of alkali (i.e. non-carbonated) and a moderate level of chloride (or chloride reaching only isolated areas of the reinforcement). The chloride ion breaks down the passive film locally in those areas where the concentration is high or the passive film is weak. A localized corrosion cell is formed with adjacent areas of passive steel acting as a cathode, where oxygen is reduced, and the anodic dissolution of iron taking place only at the small central anode. Several factors then maintain or aggravate the development of the existing pit rather than to spread the corrosion or nucleate new pits. Acid is produced at the anode (pit site) due to hydrolysis reactions and alkali at the cathode due to the reduction of oxygen. Under the acid conditions present, the corrosion products formed are soluble. Therefore, considerable amounts of corrosion can occur without spalling of the concrete. In pitting corrosion access of oxygen is the major factor in determining the total amount of corrosion. However, with the large cathode/anode area ratio, intense pitting can result even with limited oxygen supply.

General corrosion

General corrosion may result from carbonation or due to the presence of large amounts of chlorides, so a large number of closely situated pits are formed. Both anodic and cathodic processes take place everywhere on the surface, and the pH shifts associated with each of these processes cancel each other.This means that the anodic dissolution takes place in a near neutral or alkaline environment, where oxygen has access. The corrosion product, in this case, is solid rust, which occupies about 4 times the volume of the metal that has been corroded. The buildup of corrosion products on the steel reinforcing bars exerts tensile forces on the concrete cover resulting in cracking and spalling.In practice, general corrosion caused by carbonation or by chlorides has different characteristics. In cases, where carbonation has penetrated deeply, the concrete is likely to be rather permeable and semi-dry, and the rate of corrosion, once it starts, is probably controlled by the relatively high

resistivity and lack of water rather than the diffusion of oxygen. The time-of wetness , known to be an important factor in atmospheric corrosion, is an appropriate measure of corrosion rate under these conditions.Conversely, corrosion in chloride-rich concrete is more often found where water is abundant and resistivity of the concrete is low. Under these conditions the diffusion of oxygen through the water- filled pores is the rate determining factor.

Macro-Cell Corrosion

Under certain conditions, it is possible for the anodic and cathodic sites to be significantly remote from each other so that the reaction products from the anode and cathode reactions do not interact. Such conditions can exist if some of the steel is in anaerobic conditions and if the concrete is sufficiently conductive (i.e low resistivity, 12 kΩcm or less) to carry the macro -cell corrosion current. Typically this occurs in a concrete member with its lower parts permanently immersed in sea-water and extending upwards through the tidal and splash zones. This may include bridge and wharf piles, and skirting panels for wharves or promenades. Under conditions of macro-cell corrosion, the cathode reaction occurs in the oxygen-rich tidal or splash zones, with no noticeable effect on the concrete.The steel, however, dissolves at the anode which will be the immersed lower part of the member, saturated with sea-water but with little or no available oxygen. The ferrous ions react with anions present in sea-water (chlorides, sulphates, hydroxides) to produce ionic compounds which form a sticky black/green colloidal paste within the concrete, often referred to as "black rust". Since this is not an expansive reaction, the colloidal corrosion products will opportunistically occupy available spaces such as voids and pores, or fracture planes if cracking is present from other causes. The colloid can slowly migrate to the surface where, if oxygen is more abundant, it may form conventional brown/orange rust stains, or it may simply be lost in the sea-water. S ince there are few outward signs of this mechanism, and although this process is generally slow, significant loss of metal can occur over time with subsequent loss of structural integrity and possible sudden, catastrophic failure. Even concrete of high quality and density can corrode by this mechanism. General corrosion cycle of uncoated steel bar in concrete is shown in **Fig 1.3.**

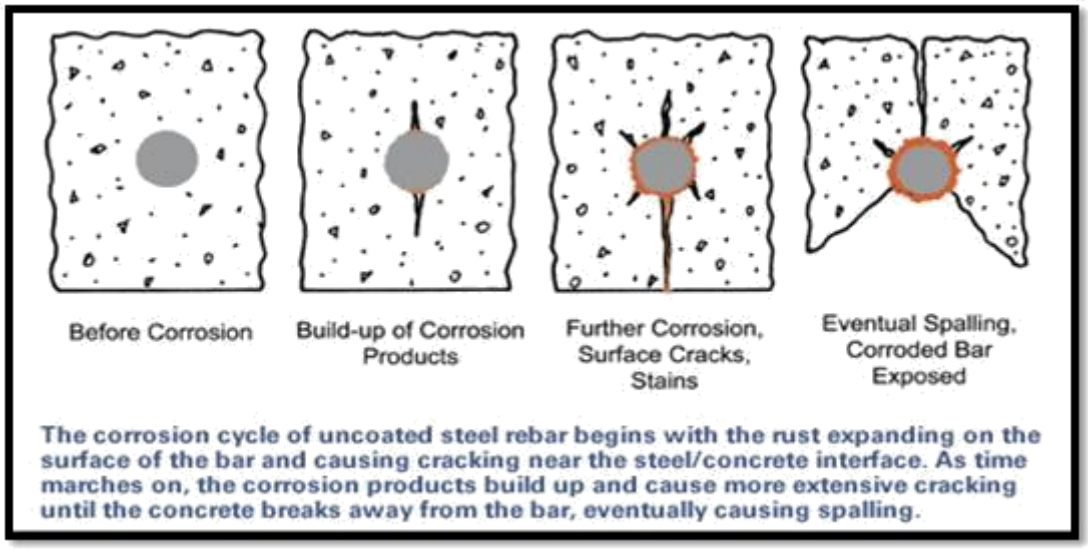

Fig 1.3 Corrosion Cycle in Reinforced Concrete (Andrade .et.al., 1996)

1.2.4 Effect on Steel

In the case of general corrosion, bond is more likely to affect structural capacity than is loss of tensile strength of reinforcement. Experiment results indicated that the level of reinforcement corrosion does not influence the tensile strength of steel bars (calculated on the actual area of cross-section), but reinforcing steel bars with more than 12% corrosion indicates a brittle failure (Almusallam A. A. 2001). Its concluded that the strength ratio and elastic modulus of reinforcement are not significantly affected by corrosion and consequently the strength and modulus of elasticity of non-corroded bars can be adopted in practice.

1.2.5 Effect on Concrete

The corrosion products have higher volume than the original steel.With the increase of corrosion level, the volume expansion of excessive rust products on the surface of steel induces radial compression pressure and hoop tensile pressure on the surrounding concrete after corrosion products fill the pores in concrete. When the hoop tensile stress exceeds the tensile strength of concrete, the concrete will crack. Hence, properties of cracked concrete should be considered to demonstrate the behavior the RC member after concrete cracks.

1.2.6 Electrochemical Methods to measure Corrosion

As a result of the development of the fundamental understanding of corrosion electrochemistry, fast and accurate potentiostats, and computer technology, a suite of electrochemical techniques exists for the study of corrosion. These techniques provide the technologist with the ability to monitor corrosion rates in service, giving early warning of conditions that could adversely affect performance and integrity. They also provide the experimentalist with the ability to determine corrosion rate with high sensitivity, assess rate controlling mechanisms, and in some cases make life predictions. Electrochemical methods are used to evaluate corrosion activity of steel reinforcement.As is the case with other nondestructive test methods, an understanding of their underlying principles and inherent limitations is needed to obtain meaningful results. In addition, an understanding of the factors involved in the corrosion of steel in concrete is essential for reliable interpretation of data from this type of testing. Three commonly used methods :-

(1) Half- cell potential
(2) Concrete resistivity
(3) Polarization resistance

Half-Cell Potential

When there is active corrosion, current flow (ion migration) through the concrete between anodic and cathodic sites is accompanied by an electric potential field surrounding the corroding bar. The equipotential lines intersect the surface of the concrete and the potential at any point can be measured using the half-cell potential method. By mapping equipotential contours on the surface, those portions of the structure where there is a high likelihood of corrosion activity are identified by their high negative potentials.

Concrete Resistivity

The half-cell potential method provides an indication of the likelihood of corrosion activity at the time of measurement. It does not, however, furnish direct information on the rate of corrosion of the reinforcement. As has been discussed, after a bar loses its passivity, the corrosion rate depends on the availability of oxygen for the cathodic reaction. It also depends on the electrical resistance of the concrete, which controls the ease with which ions migrate through the concrete between anodic and cathodic sites. Electrical resistance, in

turn, depends on the microstructure of the paste and the moisture content of the concrete. Thus, measurement of the resistivity of the concrete is useful in conjunction with a half-cell potential survey. The resistivity is numerically equal to the electrical of resistance (in ohms) times length

.

Polarization Resistance

The polarization resistance technique is a well-established method for determining corrosion rate by using electrolytic test cells. The technique basically involves measuring the change in the open-circuit potential of the short-circuited electrolytic cell when an external current is applied to the cell. For a small perturbation about the open-circuit potential, there is a linear relationship between the change in voltage ΔE and the change in applied current per unit area of electrode Δi. The ratio $\Delta E/ \Delta i$ is called the polarization resistance *Rp*. Because the current is expressed per unit area of an electrode that is polarized, the units of *Rp* are ohms times area.Each method provides distinct information related to the corrosion status. The half-cell potential provides an assessment of the likelihood that there is active corrosion in the structure. It does not, by itself, provide information on the corrosion rate. One of the controlling factors for corrosion rate is the concrete resistivity, and measurement of concrete resistivity is a useful complement to the half-cell potential survey. The polarization resistance technique allows measurement of half-cell potential along with the actual corrosion current. The latter can be used to estimate the rate of section loss of the bar. It is emphasized that any of these measurements represent the conditions at the time of testing

1.2.7 Effectiveness of Impressed Current Technique to Stimulate Corrosion of Steel Reinforcement in Concrete

Accelerated corrosion by means of the impressed current technique is widely used in concrete durability tests. The impressed current technique in accelerated corrosion studies is used so that tests can be completed within a reasonable amount of time. Corrosion is induced by applying an electrochemical potential between the reinforcing steel anode and cathode. The potential applied is varied, in order to achieve a constant applied current density. The majority of previous studies have used current densities that are from 3 to 100 times greater than the maximum current densities reported from field studies . The applied impressed current densities have typically ranged from 200 to 3,000 mA/cm2,

with a maximum of 10,400 mA/cm2 and a minimum of 45 mA/cm2.(Maaddaway. et.al.,2003) A summary of some of the previous accelerated corrosion tests on reinforced-concrete members is presented in Table1.2. Although accelerated corrosion using an impressed current is typically used, there is little information in the literature on the influence of varying the current density level on the effects of reinforcement corrosion in concrete structures.

Table 1.2 Summary of Some Previous Accelerated Corrosion Tests (Maaddaway et.al. 2003)

Table 1. Summary of Some Previous Accelerated Corrosion Tests

Study	Specimen type	Applied current (mA)	Current density ($\mu A/cm^2$)	Cathode type	Corrosion environment
Uomoto et al. (1984)	Beams	167	200–630	External copper plate	Constant immersion, 5% NaCl solution
Tachibana et al. (1990)	Beams	1,000[a]	500	External copper plate	Constant immersion, 3.3% NaCl solution
Al-Sulaimani et al. (1990)	Beams	Varies	2,000	External stainless steel plate	Constant immersion, salted solution[c]
Lee et al. (1996)	Beams	1,000	2,000[a]	External copper plate	Constant immersion, 3% NaCl solution
Lee et al. (1997)	Beams	672	230[a]	External copper plate	Constant immersion, 3% NaCl solution
Phillips (1991)[b]	Slabs	1,800 (average)	600 (average)	External steel mesh	Constant immersion, 3% NaCl solution
Almusallam et al. (1996a)	Slabs	2,000	3,000	External stainless steel plates	Specimen soffits in contact with 5% NaCl solution
Tachibana et al. (1990)	Bond pull-out	32	500	External copper plate	Constant immersion, 3.3% NaCl solution
Al-Sulaimani et al. (1990)	Bond pull-out	Varies	2,000	External stainless steel plate	Constant immersion, salted solution[c]
Almusallam et al. (1996b)	Bond pull-out	400	10,400[a]	External stainless steel plate	Constant immersion, 3% NaCl solution
Bonacci et al. (1998)[b]	Columns	150 (average)	45 (average)[a]	Internal stainless steel bar	2.5 day dry, 1 day immersion cycle in 3% NaCl solution. Concrete cast with 2% NaCl by weight of cement

1.3 Structural health monitoring (SHM)

Structural Health Monitoring (SHM) is a key development that is driving a revolution in smart-structures technologies. Promising quantum gains in the performance and cost- effective maintenance of high-value assets such as aircraft, civil infrastructure, and Structural Health Monitoring technology will be an integral component of an increasing number of future engineering structures. The rapid advances that have been made in the past two decades in sensor technology, multifunctional materials and innovative structural concepts are now leading into the practical use of Structural Health Monitoring.(Wilbur et al.,2000)

Structural Health Monitoring (SHM) is a highly interdisciplinary area of research focused on developing techniques to detect damage in structures such as buildings, bridges,

aircraft, ships and spacecraft. Most Structural Health Monitoring research to date has focused either on global damage assessment techniques using low-resolution measurements of a structure's response to ambient excitation, or on limited independent damage detection mechanisms.

Structural health Monitoring is defined as the acquisition, validation and analysis of technical data to facilitate life cycle management decisions. (Kessler et al. 2002),

Structures are assemblies of load carrying members capable of safely transferring the superimposed loads to the foundations. They are constructed (e.g. buildings, bridges, dams, transmission towers, etc.) or manufactured (e.g. machines, trains, ships, aircraft, etc.) to serve specific functions during their design lives. Each structure forms an integral component of civil, mechanical or aerospace systems. In order to serve their designated functions, the structures must satisfy both strength and serviceability criteria throughout their stipulated design lives. However, with the passage of time, some amount of deterioration and damages are bound to occur, due to a variety of factors; such as environmental degradation, fatigue, excessive loads, and natural calamities or simply due to long endurance combined with intensive usage. Even the best designed structures, constructed from advanced high strength materials, are not 100% immune from damage.To ensure structural integrity and hence maintain safety, in service health and usage monitoring techniques are employed in many engineering areas. Structural health is directly related to structural performance and in this respect it is one of the major parameter with regard to safety operation. This aspect of structural health is particularly relevant to civil structures. A number of different definitions can be proposed to describe damage, health and monitoring of structure. Intuitively, health is the ability to function /perform and maintain the structural integrity throughout the entire lifetime of the structure, monitoring is the process of diagnosis and prognosis, and damage is a material, structural or functional failure. In this context damage detection/monitoring and structural health monitoring have the same meaning.Structural health Monitoring is a new and exciting field .SHM philosophies should be applied to two families of structural components. Structural health, or equivalent, the state of damage can be established either directly or indirectly.(Yong. et. al., 2006)

Direct approach: The first approach checks for the damage type (e.g. cracks, corrosion or delamination) by applying an appropriate inspection technique. These techniques, based on

physical phenomenon, in fact sometimes also amount to response measurements but in this case they have a very local and direct character. The established inspection techniques vary from visual inspection by the naked eye to passing the structure through a fully automated inspection gantry.

Indirect approach: In this approach structural performance or rather structural behaviour is measured and compared with the supposedly known global response characteristics of the undamaged structure. If the effect of certain damages on structural response characteristics is known, this approach provides an indirect measure of damage and of structural health.

1.3.2 Techniques for SHM

Structural Health Monitoring (SHM) is estimating the state of structural health, or detecting the changes in structure that affect its performance. Two major factors are-

Techniques for SHM are given below:

1. Local Technique

2. Global Technique

1.3.2.1 Local Techniques

Structural Health Monitoring is organized around the various sensing techniques used to achieve structural health monitoring. The main emphasis is on sensors, signal and data reduction methods and inverse techniques, allowing the identification of the physical parameters, affected by the presence of the damage, on which diagnostic is established. Structural Health Monitoring is not oriented by the type of applications or linked to special classes of problems, but presents the broader families of techniques: Another category of damage detection methods is formed by the so-called local methods based on either visual inspection or different non destructive testing (NDT) methods .Most of the NDT techniques were developed in the early to mid–1960s.(Song and Saraswathy.,2006)

1.3.2.2 Methods for Local Techniques

A number of theoretical models and simulation/analytical techniques were developed in1970s. Some of the methods are given below:-

1.Visual testing

2.Ultrasonic testing

3.X ray analysis

4.Concrete resistivity
measurements 5.Cover thickness

6.Surface potential

7.Linear polarization technique
8.Galvano static pulse transient method

.

Visual Inspection*:* This technique is based on structural analysis of the concrete surface with the help of binoculars or directly through eyes, once a month, an year or once in several years depending on the importance of structure. It uses visual information such as cracks, spalled concrete cover, rust stains, exposed reinforcement, etc. as a measure of corrosion monitoring. This method is not reliable as it is possible that corrosion has been initiated on reinforcing steel, but the symptoms on concrete surface are not visible yet. It might be too late when the symptoms are visible and the structure is severely damaged. Hence, this technique fails to detect corrosion at an early stage. (Song and Saraswathy, 2007)

Ultrasonic Pulse Velocity (UPV) Measurements: Ultrasonic refers to sound energy above the audible frequency of 20 kHz. UPV is a non-destructive technique that can be used to predict material strength and detect internal damage in the structure such as cracking, decay, voids, honeycomb, etc. This technique is readily applied to the concrete structures and is very efficient in finding out the areas of weak concrete in a generally sound RC structure. In this method, electrical energy is converted into pulses of longitudinal, elastic stress waves by a transducer that is in direct contact with the concrete surface to be tested. A good contact between the transducer and concrete surface is made by using a coupling gel. The acoustic pulses generated by the transducer traverse through the concrete and after reflection, the pulses are received by transducer and converted back to electrical energy. The time taken by the wave to travel through the structure and reflect back is measured by electronic means and this is used to calculate the parameter “pulse velocity”.

Pulse Velocity, V= L/T _ _ _ _ _ _ _ _ _ _ _ _ _ _ _ (1.1)

The value of pulse velocity determines the quality of concrete.

X-ray/Gamma Radiography: Radiography technique provides useful information about concrete quality and defects within RC Structure. It uses radioactive isotopes for concrete testing. This technique is classified into X -ray radiography and γ-ray radiography, based on the em wave used for corrosion monitoring. The X -rays and γ- rays provide a radiographic examination of concrete to locate internal cracks, voids and variation in concrete density.

Concrete Resistivity Measurement: It is a NDT technique that evaluates corrosion risk on the reinforcement based on electrical resistivity measurements. The parameter "electrical resistivity" plays an important role in determining the intensity of corrosion. Greater the electrical resistivity of concrete material, slower will be the corrosion process. It has been reported that electrical resistivity is inversely proportional to the corrosion rate. Electrical resistivity is an important parameter that provides useful information about corrosion performance of steel embedded in concrete. **Fig.1.4** shows the circuit for electrical resistance measurements.

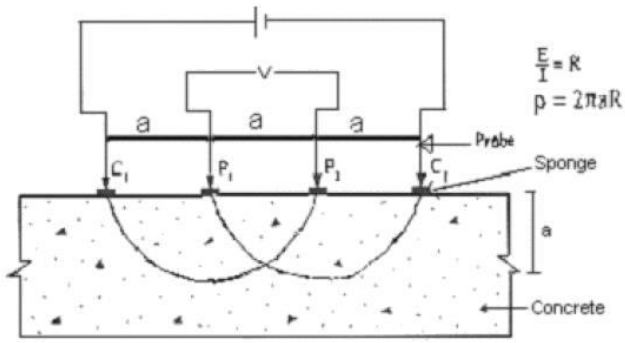

Fig 1.4: Circuit for electrical resistance measurements
(Song and Saraswathy,2007)

Cover Thickness Measurement: This NDT technique employs a device known as cover meter to measure the concrete cover for detecting rebar size, position and direction. **Fig.1.5** shows a cover meter to monitor corrosion of reinforcing steel:

Fig 1.5: Cover meter (Song and Saraswathy, 2007)

The parameter used by the cover meter is "cover thickness". This parameter is essential to preserve the electrochemical stability of steel embedded in concrete contaminated by chlorides.

Surface Potential Measurement: SP measurement is a useful technique to identify the anodic and cathodic regions in a RC structure and determines the probability of corrosion reinforcement indirectly. During corrosion process, electric current flows from anode to cathode, i.e., from higher potential to lower potential.SP measurements are based on measuring the potential dro p from anode to cathode. The schematic representation of SP Measurement is as shown in **Fig. 1.6** below:-

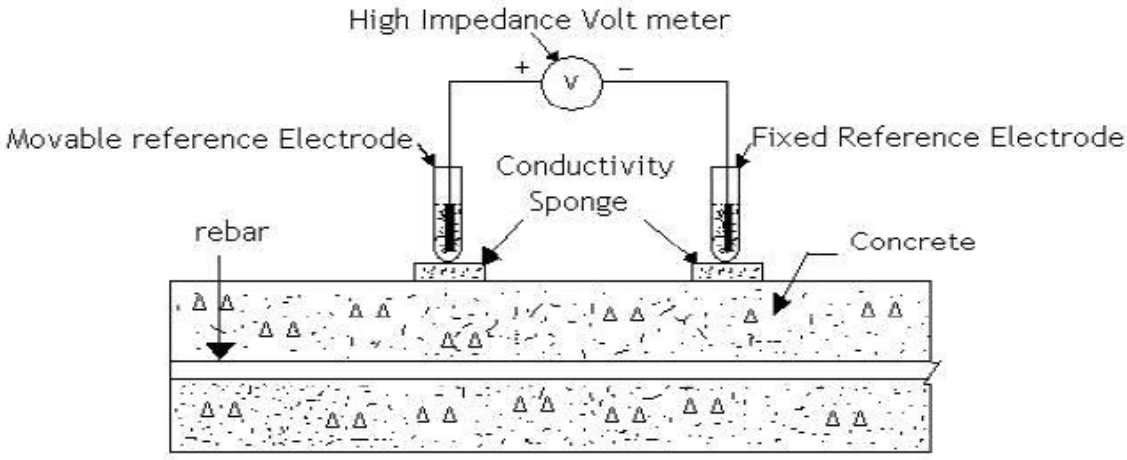

Fig 1.6: Schematic representation of surface potential (SP) measurements (Song and Saraswathy, 2007)

Two reference electrodes are shown in the above figure - a movable reference electrode and a fixed reference electrode. The moving electrode moves on the structure and measures a potential against the standard fixed electrode. The probability of corrosion is determined by

the potential difference measured between anode and cathode. The more the potential difference, more is the probability of corrosion.

Linear Polarization Resistance (LPR) Measurements: It is a useful NDT technique that determines the instantaneous corrosion rate of reinforcing steel. **Fig 1.7** shows the schematic representation of Linear Polarization Resistance (LPR) Measurement. This method provides more detailed information as compared to simple potential survey. Moreover, it is rapid, non-intrusive and enables accurate assessment of the condition of RC structures. However, this technique requires localised damage on the concrete cover in order to enable a concrete connection to the reinforcing steel. In this method, the potential of reinforcing steel is c hanged by a fixed amount ΔE and the current ΔI is monitored after a fixed time period . The change in potential ΔE should be between 10 – 30 mV (Stern-Geary range).

The polarization resistance,is given as:

$= \Delta E / \Delta I$ _ _ _ _ _ _ _ _ _ _ _ _ _ _ _ _ _ _ (1.2)

The corrosion rate, I_{corr} is expressed in terms of polarisation resistance

(1.3) $I_{corr} = B/$ _ _ _ _ _ _ _ _ _ _ _ _ _ _ _ _ _ _ (1.4)

where, B is Stern–Geary constant. B = 25 mV (for active steel)

B = 50 mV (for passive steel)

The value of corrosion current gives an indication of the condition of rebar.

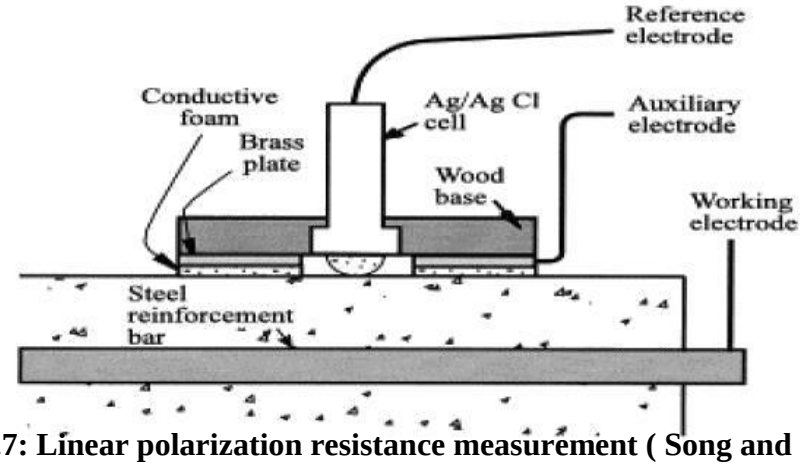

Fig. 1.7: Linear polarization resistance measurement (Song and Saraswathy, 2007)

Galvanostatic Pulse Transient Method: It is a NDT technique based on transient polarization that operates in time domain. In this method, a short time anod ic current pulse (10-200 μA) is imposed on the reinforcing steel by a counter electrode placed on the surface

of concrete. This leads to polarization of the reinforcement with respect to its free corrosion potential in anodic direction. The resulting potential difference is recorded by a reference electrode as a function of polarization time. The set up for galvanostatic pulse technique is as shown in **Fig 1.8** A limitation of this technique is that the pulse response must be stabilized to give an accurate value of potential.

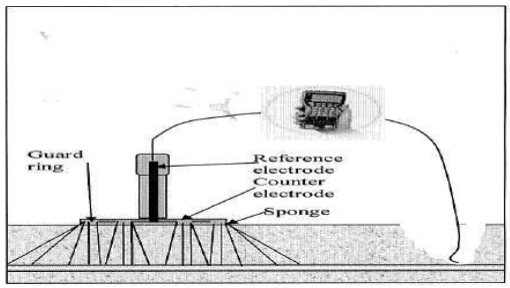

Fig 1.8: Set-up for galvanostatic pulse technique (Song and Saraswathy, 2007)

Electrochemical Impedence Spectroscopy (EIS): EIS is a very powerful and useful NDT technique that can evaluate the corrosion rate of steel over a wide range of frequencies. In this method, an alternating voltage of about 10 -20 mV is applied to rebar and the resulting current and phase angle are measured at various frequencies. EIS involves a parameter Z, Impedence which is the ratio of ac voltage to ac current. The variation of impedence with frequency is studied and is used to determine the equivalent electrical circuit which gives the same response as the given corrosion system. Although AC- EIS technique gives more information than DC-LPR measurements, but it is a very time consuming procedure, and is confined to labs instead of structures.

1.3.2.3 Global Techniques

The global SHM techniques are using the dynamic characteristics of the structure to identify the damage, its approximate location and its severity, reducing the need for manual inspection. Global techniques are very attractive to civil engineers because they can be used without direct access to structural member and no previous knowledge of damage of structure is needed, reducing the time and cost to assess the damage in structure.

In **global** techniques, the test-structure is subjected to low-frequency excitations, either harmonic or impulse, and the resulting vibration responses (displacements, velocities or accelerations) are picked up at specified locations along the structure.(Kim.et.al.,2005)

1.4 Global Analysis Using Vibration Measurements

As the cracks initiation and propagation may occur at loads far below those for actual structural failure and, in the early stages it is possible to detect using visual inspection and other conventional means. However, vibration measurements are thought to be sufficiently sensitive to detect and monitor damage even when cracks are located well within a structure. A number of vibration based parameters have been used for structural health monitoring.The basic idea behind this technology is that modal parameters i.e. frequencies, mode shapes, and modal damping are the function of the physical properties of the structure which include mass, damping, and stiffness. Therefore change in the physical properties will cause detectable changes in the modal properties. Previous studies show that the modal shapes and damping can be used to detect damage.

Vibrational Signature

Vibration based structure health monitoring have been widely developed over the years to detect the damage in RC structures . Structural diagnosis by measuring and analysing vibrational signals of any structure is a well known method. This approach first defines the baseline vibrational characteristices of a structure before damage occurs. If the new vibrational signature obtained during a routine operation deviates from baseline value than the structure should be checked for defects. This is called Vibration Signature technique. As damage normally associates with the stiffness of the structure, natural frequencies of structure will also change and hence these are the parameters most commonly used for damage detection.(Yong et al., 2006)

The usual aim of vibration measurement is to predict response to given force or moment in different damage states (Baghiee et al., 2009; Burgueno et al.,2001). For stationary structures, the specific frequencies at which resonant amplitudes occur are called the natural frequencies of the structure, and these frequencies and the corresponding distribution of amplitude are global properties. The amplitude distributions at the natural frequencies and modes of vibration are known as the natural modes of vibration.Vibration responses of structures are related to structural weaknesses associated with resonance behavior, e.g., natural frequencies being excited by operational forces. It can be shown that the complete dynamic behavior of a structure in a given frequency range can be viewed as a set of individual modes of vibration. Each result has a characteristic natural frequency, damping, and mode shape. By using these so-called modal parameters to model the structure,

problems such as specific resonances can be examined and subsequently solved. The first stage in modeling the dynamic behavior of a structure is to determine the modal parameters as introduced above:

(iv) The resonant frequency or natural frequency
(v) The structural damping
(vi) Frequency response functions
(vii) The mode shape

The modal parameters can be determined from a set of frequency response measurements between a reference point and a number of measurement points. Such a measurement point is usually called a degree of freedom (DOF).

We record dynamic characteristics from OROS 8.0 NV gate solutions by striking the hammer just above the accelerometer. These dynamic characteristics include: Triggering, FRF records are explained below:

Triggering: - Triggering is a technique for capturing an event for which it is not known exactly when it will occur. A trigger can start data acquisition and processing when a user specified voltage level is detected in and input channel. For example, we can set up a trigger to capture a hammer impact. After the trigger is armed, the analyzer will wait until the impact occurs before it starts acquiring data.

Frequency Response Function (FRF):- FRF is computed from two signals. It is sometimes called a "transfer function". The FRF describes the level of one signal relative to another signal. It is commonly used in modal analysis where the vibration response of the structure is measured relative to the force input of impact hammer or shaker. The estimation of FRF depends upon the transformation of data from time to frequency domain. The Fourier transform is used for this computation. Unfortunately, though, the integral Fourier transform definition requires time histories from negative to positive infinity. Since this is not possible experimentally the computation is performed digitally using a Fast Fourier Transform (FFT) algorithm which is based upon only a limited time history. In this way the theoretical advantages of the Fourier transform can be implemented in a digital computation scheme.

Fast Fourier Transform (FFT):- It is the discrete Fourier transform of a block of time signal. It represents the frequency spectrum of the time signal. It is a complex signal meaning that it has both magnitude and phase information.

1.5 Objectives and Scope of Work

The objective of this thesis is to study how progressive corrosion is detrimental to reinforced concrete beams.Corrosion monitoring based on visual inspection was done to detect the cracks caused due to corrosion by naked eye. Specifically, the aim is to study the effect of corrosion on the static parameters of load carrying capacity of beams and deformation characteristices and dynamic properties of beam using vibration based health monitoring subjected to corrosion at different levels. Natural frequency and maximum amplitude of control beam and beams subjected to different levels of corrosion were studied.The effect of different levels of reinforcement corrosion on static and dynamic parameters is investigated.

1.6 Closing Remarks

Followed by brief introduction of the topic this chapter introduces the effect of corrosion on RC structures its mechanism,types of corrosion and discussion on various structural health monitoring techniques with emphasis on vibration monitoring. It further discusses the objective behind the thesis and scope of work.

CHAPTER -2
LITERATURE SURVEY

2.1 Literature review on effect of corrosion on RC structures

Steel reinforcement corrosion is a major cause of dete-rioration of concrete structures in aggressive environ-ment. Steel corrosion in concrete leads to cracking, rust, spalling of the cover zone, reduction of bond strength, reduction of steel cross-section and loss of ser-viceability. Reinforced concrete undergoing corrosion does not only give the appearance of poor performance,but also can in extreme cases, lose its structural integrity. This chapter explains the work of some researchers on various effects of corrosion on the health of reinforced concrete structures on static and dynamic properties of RC beams.

El-Maaddawy et al., (2003) studied the influence of **varying the impressed current density** level between 100 and 500 mA/cm2 on the actual degree of steel reinforcing bar corrosion as well as on the concrete strain behavior due to expansive corrosion products was experimentally investigated. Twelve reinforced-concrete prisms (150x250x300mm) were used. The prisms were reinforced by two No. 10 reinforcing bars. Corrosion was induced by means of impressed current using electric power supplies. To depassify the steel reinforcement, 5% NaCl by weight of cement was added to the concrete mix. The strain response due to the expansion of corrosion products was measured at each face of the prisms.

Fig 2.1 General view for accelerated corrosion (Maaddawy et al., 2003)

At the end of the corrosion phase, all the corroded reinforcing bars were removed, cleaned according to the ASTM G1-90 standard, and weighed to get the actual degree of mass loss. The results showed that, up to 7.27% mass loss, accelerated corrosion using the impressed current technique was effective in inducing corrosion of the steel reinforcement in concrete.

With respect to Faraday's law, the use of different current densities has no effect on the percentage of mass loss. However, increas ing the level of current density above 200 mA/ cm2 results in a significant increase in the strain response and crack width due to corrosion of the steel reinforcement.

El-Maaddawy et al., (2005) studied the **flexural behaviour of corroded RC beams** under combined effect of corrosion and sustained loads. Test results showed that the presence of a sustained load and associated flexural cracks during corrosion exposure significantly reduced the time to corrosion cracking and slightly increased the corrosion crack width. For example they found that crack width would propagate 22% faster in loaded conditions. They observed that with 8.9% and 22.2% mass loss, strength losses of 6.4% and 20.0%, respectively. It was also observed that the presence of flexural cracks during corrosion exposure initially increased the steel mass loss rate and, consequently, the reduction in the beam strength. El-Maaddawy et al. (2005) concluded that at low corrosion levels, the effect of bond loss can be ignored and that the ultimate load carrying capacity of the beam is affected only by the loss on steel reinforcement.

Joyce.T.A.,(2008) carried out experiments to study the **Effect of reinforcement corrosion on flexure beahviour of RC beams.** The corrosion of steel was isolated in the flexural region in order to eliminate contributions from stirrup corrosion and loss of bond within the development length.it was determined that the flexural capacity of beams decreases as level of corrosion increases.

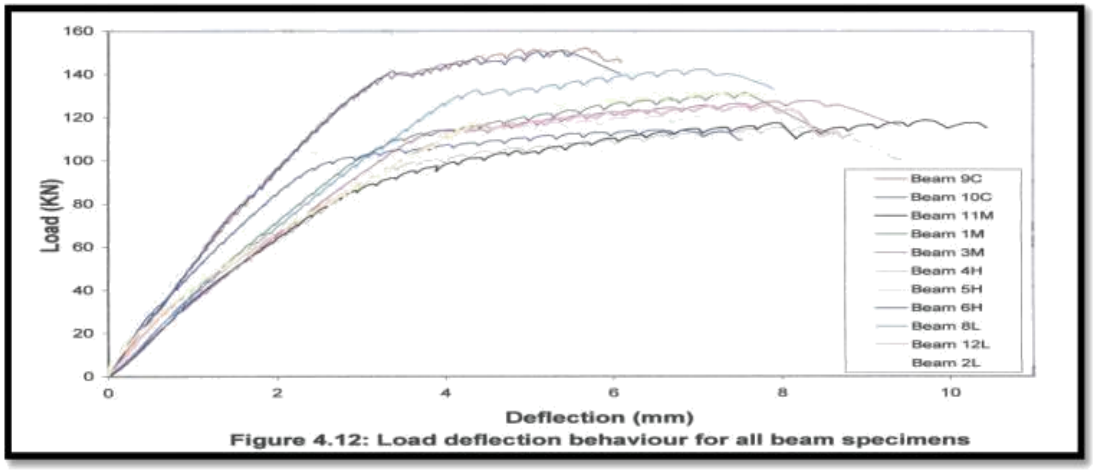

Fig 2.2 Load Deflection Behavior for all beam specimens (Joyce, 2008)

In addition to the study of flexural capacity, the prediction of the flexural behavior of corroded beams was studied through the stiffness effects of reinforcement corrosion. The stiffness study indicated a sharp drop in stiffness at relatively low degrees of corrosion, followed by a slower decline at increasing levels of corrosion. Mass loss, crack width and chloride ion content were examined as indicators of degree of corrosion.

Malumbela et al., (2009) studied the **flexural behaviour of corroded RC beams under combined effect of corrosion and constant sustained loads**. An accelerated corrosion process using a 5% solution of NaCl and a constant impressed current induced corrosion on tensile steel bars. They tested four RC beams, each with a width of 153 mm, a depth of 254 mm and a length of 3000 mm.

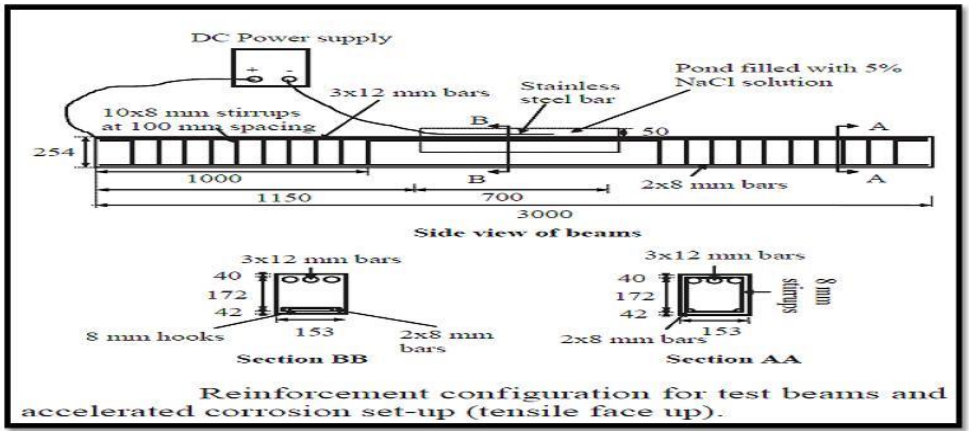

Fig 2.3 Reinforcement configuration for test beams and accelerated corrosion Setup(Malumbela et al.,2009)

Four beams were used in the test programme. Beam 1 was tested under self-weight; Beam 2 was tested under a constant sustained load that was equivalent to 10% of the ultimate load capacity of the beam (uncracked condition); and beams 3 and 4 were tested under a constant sustained load that was equivalent to 33% of the ultimate load capacity of the beam (cracked condition). Beams 1 to 3 were corroded under their respective loading systems whilst beam 4 was not corroded

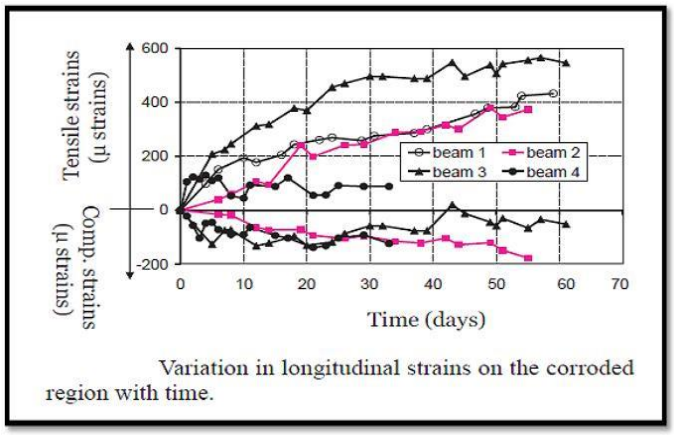

Fig 2.4 Variation in longitudinal strains on the corroded region with time. (Malumbela et al., 2009)

Fig 2.4 above shows that longitudinal tensile strains on a beam that had transverse cracks from applied load (beam 3) are higher than strains on corroded beams without flexural cracks (beams 1 and 2). After 55 days of corrosion, tensile strains on beam 3 were about 1.5 times higher than strains on beams 1 and 2. Unexpectedly, tensile strains on beams 1 and 2 were almost the same but significantly higher than strains on beam 4. Measured strains indicate that; 1. Longitudinal tensile strains are influenced by the applied load but mostly by the level of corrosion of steel bars. 2. Longitudinal tensile strains of corroded beams increase monotonically with time at a decreasing rate. **Fig 2.5** below shows that depth of the neutral axis is independent of the level of corrosion for beams free from flexural cracks and beams free from corrosion but significantly reduces with an increase in degree of corrosion for corroded beams with flexural cracks as shown below.

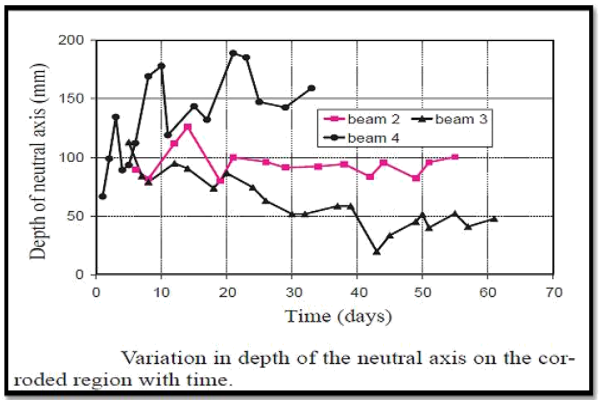

Fig 2.5 Variation in depth of the neutral axis on the corroded region with Time (Malumbela et al.,2009)

Fig 2.6 below shows that curvatures of corroded beams increase monotonically with degree of corrosion but at a decreasing rate.

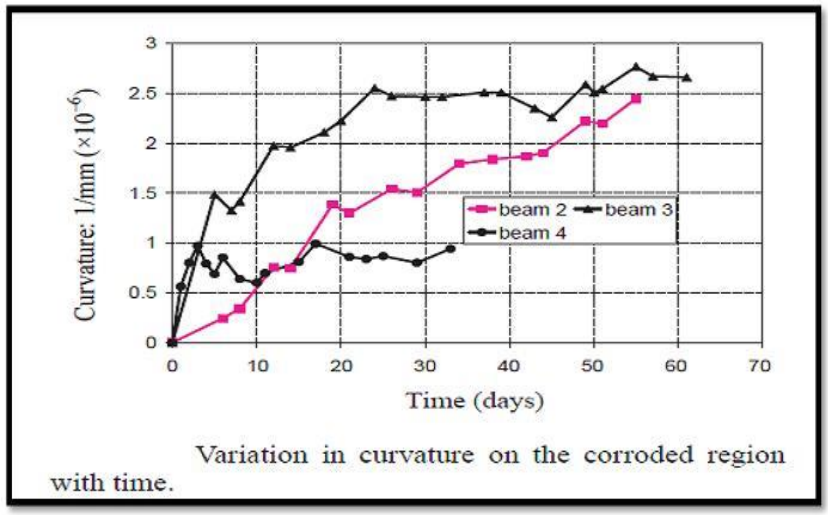

Fig 2.6 Variation in curvature on the corroded region with time. (Malumbela et al., 2009)

Fig 2.7 shown below conclude that:

1. The effective moment of inertia of corroded beams decreases monotonically with time of electrolysis but at a decreasing rate.

2. For corroded beams, the effective moment of inertia of beams with flexural cracks is almost the same as the effective moment of inertia of beams free from flexural cracks

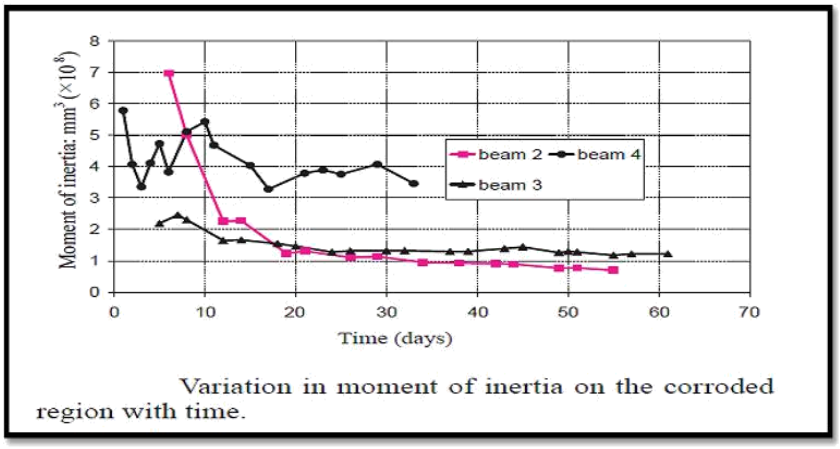

Variation in moment of inertia on the corroded region with time.

Fig 2.7 Variation in moment of inertia on the corroded region with time (Malumbela et al.,2009)

At the end it is said that the longitudinal strains, depth of the neutral axis and curvature depend on both the level of corrosion and the applied load whilst the moment of inertia only depends on the level of corrosion.

Acosta et al., (2004) studies the **influence of corrosion on structural stiffness of reinforced concrete beams**. This work presents an experimental investigation that correlates the stiffness changes of reinforced concrete beams with the amount of steel cross section loss and concrete cover cracking morphology due to localized corrosion of the embedded steel. Ten concrete beams (100 by 150 by 1,500 mm) with the central portion contaminated by chlorides placed during mixing of the concrete were used in this investigation. In addition, two beams without chloride contamination were used ascontrols. Corrosion was further accelerated in the chloride contaminated beams by impressing an anodic current to the single no. 3 steel reinforcement bar (10 mm diameter. To determine the effect of corrosion- induced stiffness deterioration, a loading-unloading technique was used. This technique was based on applying gradually (in steps) a vertical force at the beam center and measuring the corresponding displacement. Three loading-unloading cycles were performed on each beam at a time every week during the entire acceleration corrosion process. Crack widths and lengths were recorded for all beams every other week. All beams, where accelerated corrosion was induced, developed surfaceconcrete cracks. The cracks were parallel to the rebar. Most of the corroding beams (7 out of 10) presented only one crack parallel to the rebar at the concrete surface closest to the rebar (bottom surface).

The results in Table 2.1 show a marked decrease in the flexure stiffness for all types of corroding beams with general corrosion (GC), localized corrosion (LC), and highly localized corrosion (HLC).

Table: 2.1 Decrease in Flexural Stiffness Acosta et. al., (2004

Experimental Values of $K(t)_{EQ}$ in KN/mm[A]

Time (days)	V01[B]	V02[B]	V03	V04	V05	V06	V07	V08	V09	V10	V11	V12
8	4.57	7.04	5.96	5.97	5.98	6.94	7.29	6.91	6.03	4.89	5.72	5.71
15	4.19	5.94	5.58	4.97	5.22	6.46	6.80	6.64	5.54	5.14	5.55	5.56
22	4.45	7.05	5.71	5.78	5.46	6.76	6.75	6.59	6.18	5.80	5.53	5.74
29	4.52	7.16	5.81	5.01	5.39	5.85	6.52	6.07	5.59	4.74	5.41	5.39
36	4.56	6.73	5.88	5.23	5.24	6.22	7.25	6.01	5.27	4.77	5.53	5.39
42	4.56	6.27	5.35	5.39	5.41	6.06	7.54	6.40	5.39	5.13	5.23	5.21
50	4.30	5.88	4.73	4.51	4.81	6.91	5.85	5.65	4.72	4.99		
57	3.99	6.27	5.24	4.96	5.33	5.83	5.74	6.22	5.21	4.89		
64	4.03	6.30	5.21	4.90	5.22	5.79	5.83	6.10	5.20	4.85		
71	4.23	6.56	4.75	4.38	5.36	5.88	5.56	5.95	5.85	4.95		
77	4.30	6.46	4.87	4.20	5.06	5.96	5.86	5.56	6.20	4.94		
88	4.15	6.46	4.76	3.91	5.43	5.48			5.26	4.52		
92	4.01	6.38	4.91	4.36	4.65	5.17			4.74	4.49		
98	4.52	6.46	4.36			4.65			4.40	4.43		
114						4.87				4.40		
128						4.47				4.24		
142						4.47				4.15		
156						1.41				3.99		
172						4.24				3.99		
181						3.82				3.99		
SL_{END}(%)[C]	1.09	8.24	26.84	26.97	22.24	44.96	19.62	19.53	27.03	18.4	8.57	8.76

[A] $K(t)_{EQ}$ = equivalent stiffness (slope obtained from the load-displacement experimental results) at time t.
[B] Control beam: beam in which there was no chloride added and no externally applied anodic current.
[C] $SL_{END} = 100 \times [K(181)_{EQ} - K(8)_{EQ}] / K(8)_{EQ}$.

The results obtained showed decreases as high as 32% in the flexure stiffness when only 14% of rebar radius was lost due to localized corrosion, for similar rebar radius loss due to corrosion (about 10%) the stiffness decreased 19.6%, 24.6%, and 26.9%, for HLC, LC, and GC, respectively.

2.2 Literature survey on Vibration monitoring

Ndambi et al., (2000) found from RC beam tests that damping increased with excitation amplitude, and that modal damping ratios were highly influenced by non- linear effects, and are, therefore, highly subjective and difficult to estimate.Damping capacity experiments of small plain mortar beams were undertaken by Wen and Chung (2000).It was found that damping increased three-fold with the embedment of steel reinforcing bars into the mortar. Damping was also increased by at least two orders of magnitude with the addition of silica fume.

Maia et al., (2002) present the subject of damage detection in structures. A series of numerical simulations on a simple beam are made in order to compare various damage detection methods based on mode shape changes. A generalization of these methods to the whole frequency ranges of measurement is proposed, i.e. methods based on mode shape changes become based on operational mode shapes. The objective of such a study is to ascertain the possibility of using various damage detection methods without the need for modal identification. He has developed some simple methods and tools based upon the use of FRF, which seem promising and have given good results in some practical applications. He also presented a new approach of FRF-based methods.

Waters et al. (2003) identified the foundation stiffness of a partially embedded post from vibration measurements. This paper investigates the behavior of beam-like structures with a view to identifying a suitable monitoring technique for post foundations. In this initial study a lighting column is modeled as a uniform rigid beam that is constrained by collocated equivalent translational and rotational springs. Expressions are derived for the equivalent spring constants as functions of foundation profile and depth. Modal and static responses are presented as functions of foundation properties. The inverse problem of identifying the foundation stiffnesses from response measurements is discussed. **Fig 2.8** shows the measured static stiffness of the beam as a function of measurement position. A simple method is proposed based on quasi-static stiffness measurements obtained from impact tests. The method is validated using measurements of a laboratory scale structure.

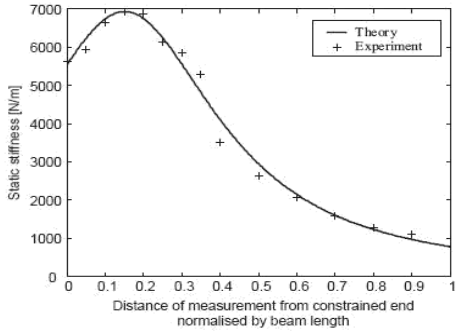

Fig 2.8. Static Stiffness of Rigid beam Constrained by two Discrete Springs (Waters et al.,2003)

Maeck et al., (2003) did damage assessment using vibration analysis on the Z24-Bridge. According to them Vibration monitoring is a useful evaluation tool in the development of a non-destructive damage-identification technique, and relies on the fact that occurrence of damage in a structural system leads to changes in its dynamic properties. It can give global information of a structure, and the location of the damage has not to be known in advance. The damage-identification technique is based on the observed shifts in eigen frequencies and mode shapes and relate the dynamic characteristics to a damage pattern of the structure. The presented technique makes use of the calculation of modal bending moments and curvatures to derive the bending stiffness at each location. The basic assumption is that damage can be directly related to a decrease of stiffness in the structure. Damage assessment techniques are validated on the progressively damaged prestressed concrete bridge Z24 in Switzerland, tested in the framework of the Brite Euram project SIMCES. They concluded that direct stiffness calculation seems to be a good alternative for other detection methods like sensitivity-based updating techniques. Despite of numerical inaccuracies at some locations of the bridge, damage was clearly observed and localized for settlements of 80 and 95 mm. For the considered bridge higher modes seem to give bad results due to more numerical inaccuracies. As a manner of improving the method, curvatures could be determined experimentally; this is under investigation at the moment. Modal curvatures are very sensitive to damage in a structure.

Jeong et al., (2005) did Vibration-based damage monitoring in model plate-girder bridges under uncertain temperature conditions. According to them the feasibility of using them for damage detection, however, is limited when their changes go undisclosed due to uncertain temperature conditions, particularly for large structures. In this paper, a vibration-based damage monitoring scheme to give warning of the occurrence, the location, and the severity

of damage under temperature-induced uncertainty conditions is proposed. Firstly, experiments on a model plate-girder bridge, for which a set of modal parameters were measured under uncertain temperature conditions, are described. Secondly, a damage warning model is selected to statistically identify the occurrence of damage, by recognizing the patterns of damage-driven changes in natural frequencies of the test structure, and by distinguishing temperature-induced off-limits. Thirdly, a frequency-based damage index method based on the concept of modal strain energy is implemented into the test structure to predict the location and the severity of damage. In order to adjust the temperature induced changes in natural frequencies that are used for damage detection, a set of empirical frequency correction formulae are derived from the relationship between temperature and frequency ratio.

Dionysius et al., (2005) studied the application of a laser Doppler vibrometers (LDV) for structural health monitoring using ambient vibration. The work covered three important issues namely, data acquisition, system identification, and structural damage detection. They concluded that the experiment investigation on bolted lap joint show the ability of the proposed methodology in locating damage in simple cases such as single location of damage by observing the maximum deviation of stiffness and damping matrices. The algorithm was also found to be effective in sizing the magnitude of stiffness, whose changes can be used as indicators for the severity of damage especially in the case of progressive damage. The importance of this study is twofold: (i) identification of modal characteristics of a structural system using ambient vibration in a non-contact manner, and (ii) detection of damage location and severity using modal information without a prior structural model. These are important features for future structural health monitoring with vibration measurement.

Hang Hao et al., (2006) did long term vibration monitoring of an RC slab with Temperature and humidity effect. They discriminate the variation of modal properties due to environmental change from those caused by structural damage, and quantify the environmental effect in vibration-based structural health monitoring and damage identification. Environmental conditions affect structural vibration properties in a complicated manner. This paper only investigates the variation of frequencies, mode shapes and damping with respect to temperature and humidity changes. A

reinforced concrete slab, which was constructed and placed outside the laboratory, has been periodically vibration tested for nearly two years.

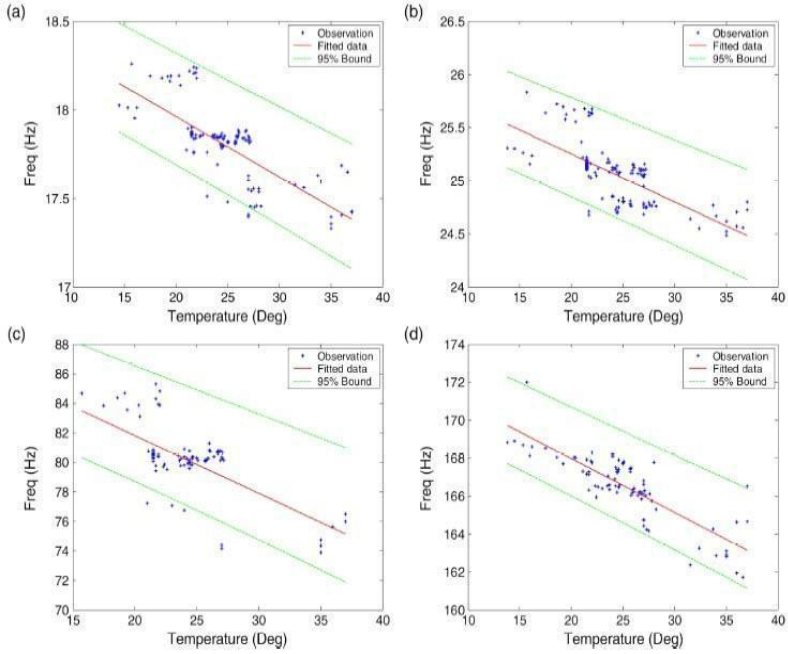

Fig 2.9(a)-(d) Relation of Frequency to Temperature Hang Hao et al. (2006)

This paper reports results obtained over that time for the first four modes. It is found that the frequencies have a strong negative correlation with temperature and humidity, damping ratios have a positive correlation, but no clear correlation of mode shapes with temperature and humidity change can be observed. in **Fig 2.9(a)–(d)** together with the 95% confidence bounds. Linear regression models between modal properties and environmental factors are built. A quantification analysis shows that variation of the elastic modulus of the material is the primary cause of the variation of modal properties.

Ha-Won Song Velu Saraswathy (2006) studied failures in the structures do still occur as a result of premature reinforcement corrosion. The maintenance and repair of bridges and buildings for their safety requires effective inspection and monitoring techniques for assessing the reinforcement corrosion. Engineers need better techniques for assessing the condition of the structure when the maintenance or repair is required. These methods need to be able to identify any possible durability problems within structures before they become serious. This paper reviews all the electrochemical and nondestructive techniques

from the point of view of corrosion assessment and their applications to bridges, buildings and other civil engineering structures.

Baghiee et al., (2009) studied damage and CFRP strengthening of RC beams by vibration monitoring. They focused on the use of mode shapes and their derivatives. The Modal Assurance Criterion and Coordinate Modal Assurance Criterion factors were used to detect damage. These factors were derived from mode shapes and modal curvatures. They found that the modal assurance criterion was subjected to very small change by damage or strengthening. The coordinate modal assurance criterion factors might detect the changes in beam stiffness at degree of freedom.

Thalapil.J, Maiti .S.K.,(2014)

This paper is an attempt to analyze the natural vibration of monolithic beams with longitudinal cracks for developing a method for its detection. An analytical method has been developed to address both forward problem of determination of natural frequencies knowing the beam and crack geometry details as well as inverse problem of detection of crack with the knowledge of changes in the beam natural frequencies. Both long (Euler–Bernoulli) and short (Timoshenko) beams have been examined numerically. For modeling a crack located at the free end of a cantilever, the beam is divided into three segments. For an internal crack located away from the free end of the beam, it is split into four segments. In both cases, two of the segments take care of beam portions above and below the crack. The cracked segments are constrained to have the same transverse displacements but different axial deformations. The modeling shows good accuracy for both the forward and inverse problems. The results thus show encouraging possibility of exploitation of the proposed method for crack detection **.**

2.3 Closing remarks

This chapter discusses about the literature survey done by various people on effect of corrosion on RC structures and study of vibration monitoring on structures

CHAPTER-3

EXPERIMENTAL INVESTIGATIONS

Main objective of the thesis was to study the behaviour of reinforced concrete beams at different levels of corrosion and its consequent effect on static and dynamic behaviour of RC beams subjected to different levels of corrosion of varying levels.To carry out the investigation, four real size beams were cast (127x227x4100)mm.Out of these four beams, one beam was kept as control beam (C-0). It was subjected to impact and its signature was taken. The other three beams (C-7,C-15,C-24) were corroded at different levels of corrosion. All three beams were corroded using impressed current technique for 7 days, 15 days and 24 days respectively representing varying degree of corrosion. The change in the crack pattern, change in dynamic properties and load deflection characteristices due to varying level of corrosion were studied.

3.1 Test matrix and program

Test program for the experimental study is as under:

1. Determinations of basic properties of constituent materials namely cement, sand, coarse aggregates and steel bars as per relevant Indian standard specifications.

2. Four real size beams were cast of size (127 x 227 x 4100mm) using M20 grade concrete.
3.Out of four beams one beam was kept as control beam and the other three beams were corroded to different levels using accelerated corrosion technique

4.. After the corrosion process was completed, vibration signature of control beam was taken and all the other three beams were also subjected to vibration monitoring, to relate the effect of varying corrosion with the dynamic behavior of RC beams.

5. All the four beams were also tested under static loading, to study the effect of varying corrosion on the load -deflection behavior of RC beams.

3.2 Materials

Cement, fine aggregates, coarse aggregates, reinforcing bars are used in casting of beams. The specifications and properties of these materials have been listed below.

Cement

Portland pozzolana cement was used for the study. The physical properties of cement as obtained from various tests are listed in **Table 3.1**. All the tests are carried out in accordance with procedure laid down in IS : 8112-1989.

Table 3.1 Physical Properties of Cement used

Sr. No	Characteristics	Value obtained Experimentally	Value specified by IS: 8112-1989
1	Standard consistency	33	-
2	Fineness of cement as retained on 90 micron sieve	1.0	<10%
3	Setting time1. Initial 2. Final	2hrs 5 hours	>30 mins <10 hours
4	Specific gravity	3.05	-

Fine Aggregates

The sand used for the experimental program was locally procured a nd conformed to grading zone II. The sand was first sieved through 4.75 mm sieve to remove any particles greater than 4.75 mm and then was washed to remove the dust. The fine aggregates were tested per Indian Standard Specifications IS : 383-1970. Properties of the fine aggregates are listed below .

Table 3.2 Sieve analysis of fine aggregate

S. No.	Sieve No.	Mass Retained (g)	Percentage retained	Percentage passing	Cumulative %age retained
1.	4.75 mm	15	1.5	99.9	1.6
2.	2.36 mm	21.5	2.15	97.75	2.25
3.	1.18 mm	204	20.4	77.35	22.65
4.	600 µm	190.5	19.05	58.3	41.7
5.	300 µm	298	29.8	28.5	71.5
6.	150 µm	225	22.5	6	94
7.	Pan	60	6	ΣF	**232**

Fineness Modulus of fine aggregate =ΣF/100=232/100=2.32

Table 3.3 Properties of fine aggregates

S. No.	Characteristics	Value
1.	Type	Uncrushed (natural)
2.	Specific gravity	2.67
3.	Total water absorption	4.9 %
4.	Fineness modulus	2.32
5.	Grading zone	II

Coarse Aggregates

Crushed stone aggregate (locally available) of 20mm and 10mm are used throughout the experimental study. The physical properties and sieve analysis of coarse aggregate are given in **Table 3.4 and Table 3.5 and Table 3.6.**

Table 3.4 Sieve analysis of 10mm aggregates

S. No.	SieveNo.	Mass retained (kg)	Percentage retained	Percentage passing	Cumulative %age retained
1.	80 mm	-	0.00	100	0.00
2.	40 mm	-	0.00	100	0.00
3.	20 mm	-	0 .00	100	0.00
4.	10 mm	1.005	33.5	66.5	33.5
5.	4.75 mm	1.572	52.4	14.10	85.9
6.	Pan	0.423	14.1	ΣC	**119.4**

Fineness Modulus of Coarse aggregate (10 mm) = ΣC+500/100 = (119.4+500)/100 = 6.19

Table 3.5 Sieve analysis of 20 mm aggregates

S. No.	Sieve No.	Mass retained (kg)	Percentage retained	Percentage passing	Cumulative %age retained
1.	80 mm	0	0.00	100	0.00
2.	40 mm	0	0.00	100	0.00
3.	20 mm	19	.633	99.367	.633
4.	10 mm	2.92	97.32	2.047	97.953
5.	4.75 mm	.035	1.17	.877	99.123
6.	Pan	.025	.833	ΣC	**197.709**

Fineness Modulus of Coarse aggregate (20 mm) = ΣC+500/100 = (197.709+500)/100 = 6.9771

Table 3.6 Physical Properties of Coarse Aggregates

SNo.	Characteristics	Value	
		20mm	10mm
1.	Type	Crushed	Crushed
2.	Specific gravity	2.63	2.60
3.	Total water absorption	1.7%	2.29%
4.	Fineness modulus	6.97	6.194

Water

Fresh and clean water is used for casting the specimens in the present study. The water is relatively free from organic matter, silt, oil, sugar, chloride and acidic material as per Indian standard.

Reinforcing bars

HYSD steel of grade Fe-415 of 10mm,8mm and 6mm diameters were used as longitudinal steel. 10mm Ø bars are used as tension reinforcement and 8mm Ø bars are used as compression steel 6mm Ø bars are used as shear stirrups. The properties of these bars are shown in **Table 3.7**

Table 3.7 Physical Properties of Steel Bars

Sr. No.	**Diameter of bars/ mesh wire**	**Yield-Strength (N/mm2)**	**Ultimate strength**	**Percentage Elongation**
1.	10mm	440.55	513.2	15.1
2.	8mm	559.5	637.23	21.6
3.	6mm	449.2	612.8	32.5

3.3 Design mix proportions of concrete

M20 grade concrete mix was used and prepared according to IS code method using the properties of materials as discussed above i.e. Table 4.1 to Table 4.6 The water-cement ratio was kept as **0.5**. The design mix proportion of the concrete were calculated as

1:1.5:2.82(cement: sand: aggregate). Total six cubes of size (150 x 150) mm were cast for the compressive strength test. Three cubes were tested after 7 days of curing and rest 3 after 28 days. The average compressive strength of materials after 7 days and 28 days comes out to be 16 and 28.5KN/m² which is acceptable..

3.4 RCC Beam Design

The beam used for experimental study is designed using limit state method (IS-456-2000). It is designed as under-reinforced section. The beam is reinforced with 2 bars of 8 mm at compression face and 2 bars of 10-mm at tension face 6mm stirrups were spaced at 150mmc/c Longitudinal section and cross-section of beam are shown in **Fig 3.1**

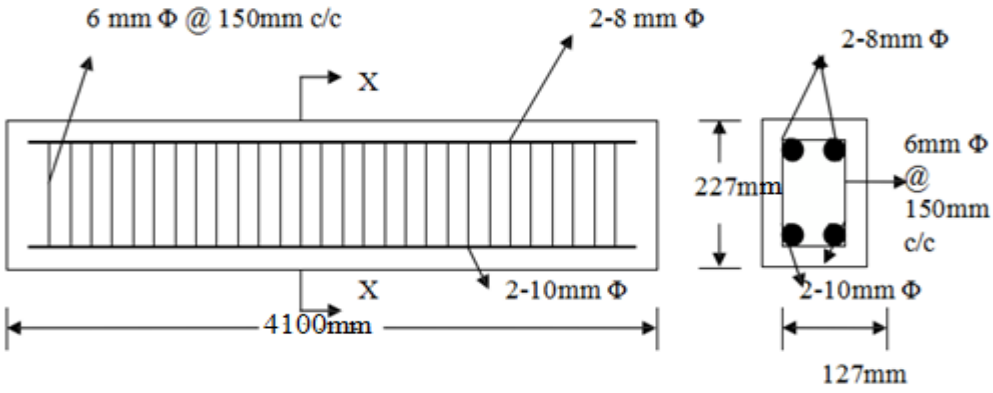

(a) L-section (b) X-section

Fig 3.1 Specimen details

3.5 Casting of Composite Beams

The casting of beams was done in single stage. The beams were cast in mould of size 127 x 227 x 4100 mm. Entire beam mould is first oiled so that the beam can be easily removed from the mould after 24 hours. Spacers of size 25mm are used to provide uniform cover to the reinforcement. When the bars have been placed in position as per design, concrete mix is poured in the mould and the beam is vibrated using a needle vibrator, to ensure the proper compaction. The vibration is done until the mould is completely filled and there is no gap left. The beams are then removed from the mould after 48 hours. After demoulding ,the beams were cured for 28 days using jute bags. **Fig 3.2** and**Fig 3.3** shows the beams before and after casting.

Fig 3.2 Beam mould with reinforcement cage **Fig 3.3 Beam after casting**

3.6 Inducing Corrosion in RC Beams

Out of all four beams, three beams were corroded using impressed current technique for 7 days, 15 days and 24 days respectively. Initially one control beam was subjected to the accelerated corrosion until the longitudinal crack spread in the whole length of the beam, which took 24 days. And then the test matrix for the corrosion was further decided. So, rest two beams were subjected to 7 days and 15 days representing different levels of corrosion. The corrosion of reinforcing steel was accelerated by impressed current technique. This was done through an integrated system incorporating a DC rectifier with a built- in ammeter to monitor the current and voltage to control the current intensity. Scientech Dual Power Supply with a maximum output of 2A at 30V was used **Fig 3.4 .** This method of corrosion was employed to reach advanced stages of deterioration in a relatively short time. At a time two beams were connected in series for corrosion process. Central 1.5 m portion of concrete beams were subjected to corrosive environment. It was done by continuous sprinkling of 3.5 % NaCl solution. This type of arrangement was selected to assure that the corrosion product formed is not washed away and cracks are formed in the concrete specimens. The direction of the current was adjusted so that the reinforcing steel became an anode and a stainless steel wire mesh wrapped all around concrete beams at centre 1.5m served as a cathode.

Fig 3.4 DC Regulated Dual Power Supply Source(constant voltage)

Fig 3.5 Stainless steel wire mesh wrapped around central 1.5 m part of Concrete beam served as cathode

3.7 Study of Load-Deflection Characteristics

After all the beams were corroded to different levels of corrosion and dynamic characteristics are studied, load -deflection behavior of beam was study to relate the effect of corrosion on RC beams. All the four beams were tested under simply supported end conditions. Ultimate load **P-Δ tests** were performed in the laboratory to determine the load-carrying capacity of the beam specimens. The loading arrangement used was four-point loading. This arrangement allows for a central region having virtually constant moment without any shear force. Hydraulic operated jack in **Fig 3.6** and corresponding Data acquisition system in **Fig 3.7** is shown below:-

.

Fig 3.6 Hydraulic operated jack

Fig 3.7 Data aquisition system

The load is applied to the beam with the help of load cell and load value is obtained from the data acquisition system, which is attached with the load cell .Two LVDT's are placed at the center and at a distance of span/4 from the end of beams to record the deflection against the loading as shown in **Fig 3.8**

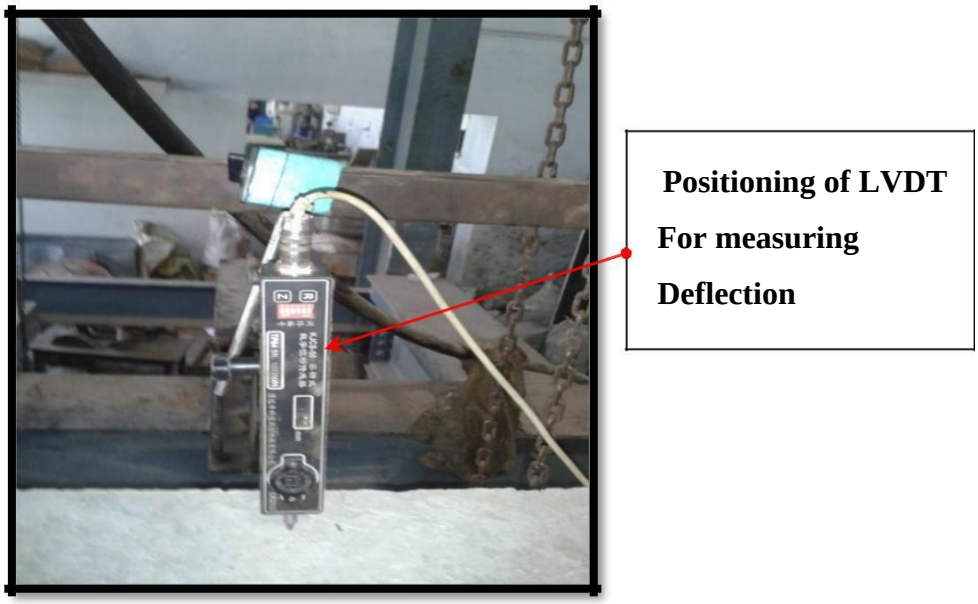

Fig 3.8 LVDT

3.8 Vibration monitoring

After all the beams subjected to different levels of corrosion, vibration characteristices of all beams were recorded using software OROS 8.0 using NV Gate solutions software.Vibration characteristices were studied on control beam and corroded beam. We recorded dynamic characteristices from FFT analyser by striking the hammer just above the accelerometer. The point for excitation was chosen as centre of beam as shown in **Fig 3.9**

Fig 3.9 Accelerometer placed below at centre postion of beam

3.8.1 Equipments used in Vibration Monitoring

Accelerometers

FFT Analyzer

Impact hammer kit

Fig 3.10 Various arrangements in software

3.9 Closing remarks

This chapter highlights the experimental procedure adopted in this research work. Firstly this chapter gives a brief introduction about the concrete mix adopted for casting of RC beams. It mainly covers the description of properties of the materials like cement, sand, aggregates and water. And based on this knowledge design mix was done. M20 grade concrete was adopted. Further this chapter covers the information about the design section adopted for RC beams and briefly describes the casting procedure of RC beams. This chapter also highlights the devices used for inducing corrosion in RC beams and for study of load deflecting behavior and vibration monitoring.

CHAPTER-4
RESULTS AND DISCUSSIONS

In this chapter, deterioration in RC beams subjected to varying degree of corrosion was studied by measuring the effect on load carrying capacity of beams, variation in crack pattern and effect on load carrying capacity and deflections under static four point loading was studied and dynamic characteristics of RC beams were also measured using Vibration monitoring subjected to different level of corrosion.

4.1 Visual Inspection

Visual inspection refers to evaluation by means of eyesight, either directly or assisted in some way. The visual inspection of a structure is the "first line of defense"and typically involves the search for large-scale deficiencies and deformities. As discussed earlier, initially one control beam was subjected to the accelerated corrosion until the longitudinal crack spread in the whole length of the beam, which took 24 days. And then the test matrix for the corrosion was further decided. So, rest two beams were subjected to 7days and 15 days of corrosion representing different levels of corrosion. So results of visual observation are discussed below in order of increasing corrosion level:-

4.1.1 Beam corroded to 7 days(C-7)

A beam undergoing accelerated corrosion for 7 days shows reddish brown patches of corrosion product on the three sides of beam at centre 1.5m portion of beam as shown in **Fig 4.1** It was noticed that no cracks were generated on surface of beam after 7 days corrosion. It was observed that at 7 days corroded beam shows small corrosion products with liquid oozes from the surface and no cracks as compared to other beam

Fig 4.1 Bottom face of C-7

Fig 4.2 Right side of front face of C-7

Fig 4. 3 Red brownish products observed along the side

4.1.2 Beam corroded to 15 days (C-15)

Beam undergoing corrosion for 15 days shows reddish brown patches on four sides at centre 1.5m portion of the beam along with cracks on bottom and side faces. At the bottom of the C-15 beam flexural crack at centre with bending of beam was observed along with red brownish colored corrosion products as shown in **Fig 4.5**. At the front side face of the beam vertical cracks were observed originating from tension face towards compression face as shown in **Fig 4.6.** At the back side face of the beam it was observed that full centre 1.5m portion of the beam was covered with reddish brown patches, and longitudinal crack was observed on the surface throughout the centre 1.5m portion of the beam. A reddish brown liquid oozes out from the sides of beam with spalling of concrete is observed on back face of beam as shown in **Fig 4.8 and 4.9**

Fig 4.4 Bottom face of C-15

Fig 4.5 Flexural crack at centre of C-15

Fig 4.6 Longitudnal and tranverse cracks at right face of C-15

Fig 4.7 Cracks on left face of C-15

Fig 4.8 and 4.9 Spalling of concrete and then complete removal of concrete cover in C-15

4.1.3Beam corroded to 24 days(C-24)

Beams undergoing corrosion for 24 days shows dark reddish brown corrosion products with reddish brown liquid oozes out from the cracks on all faces of the beam at centre 1.5m portion. Corrosion products formed in C-24 beam was in large volume than in other cases. At the front face of C-24 beam big vertical crack was observed throughout the centre1.5m portion of the beam as shown in **Fig 4.10** results into breaking of beam from the center part. At the front side face also longitudinal crack was observed throughout the centre 1.5m portion along the tension bar as shown in **Fig 4.11**.At the back face small vertical and horizontal cracks were observed with major vertical crack at centre. At the bottom face of beam large corrosion products were noticed but no major crack generated. It was noted that deterioration of C-24 beam due to corrosion was more than the other beams.

Fig 4.10 Long vertical crack at centre of beam results in breaking of beam

Fig 4.11 Dark reddish brown corrosion products

Fig 4.12Long horizontal cracks at the bottom side of front face

4.2 Load Deflection behaviour of RC beams

After the corrosion process was completed, all beams including control beam tested for load deflection behaviour. Beams were loaded in four-point bending until failure and the corresponding load and deflections at midspan and span/4 were measured using LVDTS.

4.2.1 Control Beam

The control beam (C-0) was tested under four point loading. The setup ensures pure bending in the central third portion of the beam. The beam was as shown in **Fig 4.13** and loads were applied till the failure and beam stop taking further load. It may be noted that the beam sections were under reinforced and steel yielded before concrete. The first crack appears at a load of 22.5KN near the left point load, accompanied by number of flexure cracks at the side face of control beam. As the load on the beam further increased the beam finally failed at 26KN. Almost all cracks were vertical near top and bottom edge, sub cracks were developed connecting to main cracks. So experimentally it was observed that ultimate load for the control beam is 26 KN with ultimate deflection at mid-span as 80.08mm and at span/4 deflection is 36mm as shown in **Fig 4.14 and 4.15** . Load deflection values and corresponding stiffness values at L/2 at different points are showed in **Table 4.1.** The load deflection response of the control un-corroded beam at L/2 and L/4 is shown in **Fig 4.14 and 4.15**

Fig 4.13 Flexure Cracks on side face of C-0 beam

Table 4.1 Load deflection values of control beam at L/2 deflection

S.No.	Load (kN)	Deflection at L/2	
		Deflection (mm)	Stiffness (N/m)
1	0	0	0
2	5	5.2	0.96
3	8	10.9	0.73
4	12.4	18	0.68
5	15.1	25	0.60
6	16.4	30	0.54
7	20	38	0.52
8	22	58	0.37
9	26	80.08	0.32

Fig 4.14 Load deflection curve of control beam control beam C-0 At L/2

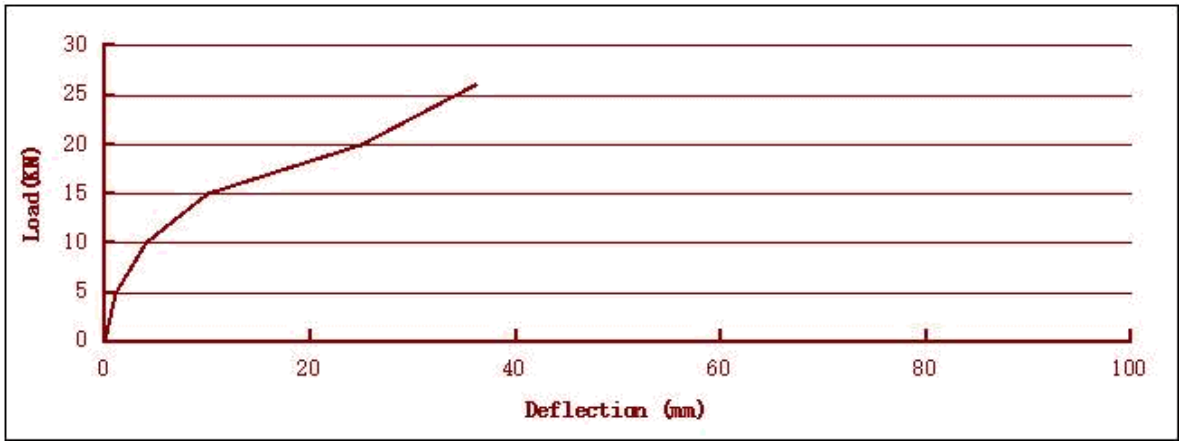

Fig 4.15 Load deflection curve of control beam C-0 At L/4

4.2.2 Beams corroded to 7 days (C-7)

Fig 4.16 shows beam with 7 days corrosion having no previous corrosion cracks as discussed earlier was tested under static loading. First crack appeared at a load of 19.02KN at centre of the beam near tension zone. Load is further increased the cracks widened and start progressing towards the compression zone and beam suddenly failed at load of 23 KN from extreme tensile face at centre as shown in **Fig 4.17**. No additional cracks appear on the surface of beam. **Table 4.2** shows load deflection values at different points and corresponding stiffness values at L/2 deflection.**Fig 4.18 ,4.19** show the graphical representation of load deflection behavior of C-7 beam. P-Δ curves indicated that there is a decrease in load carrying capacity and deflection capacity as compared to control beam. It was noticed from the results that there is decrease in load carrying capacity of C -7 beam as compared to control beam.

Fig 4.16 Side face of C-7 Beam before load

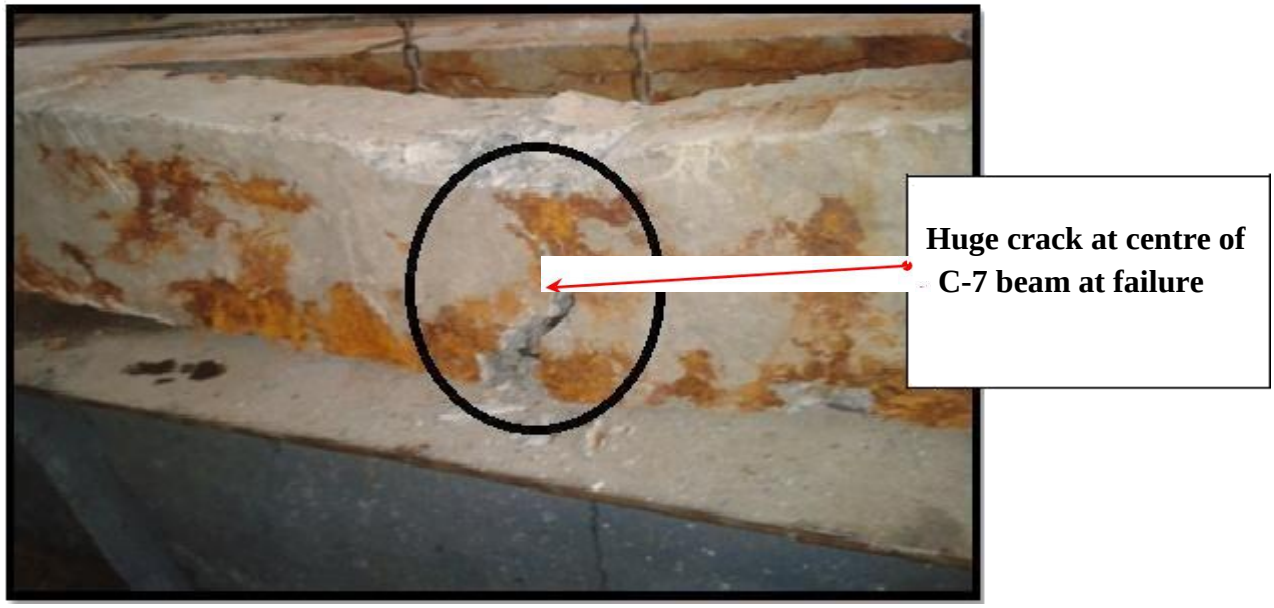

Fig 4.17 C-7 Beam showing huge crack at centre after failure

Table 4.2 Load deflection values of beam subjected to 7 day corrosion

S.No.	Load (kN)	Deflection at L/2	
		Deflection (mm)	Stiffness (N/m)
1	0	0	0
2	5	6	0.83
3	8	11	0.72
4	12	20	0.6
5	15.5	27	0.57
6	17	30	0.56
7	20	42	0.47
8	21	55	0.38
9	23	74	0.31

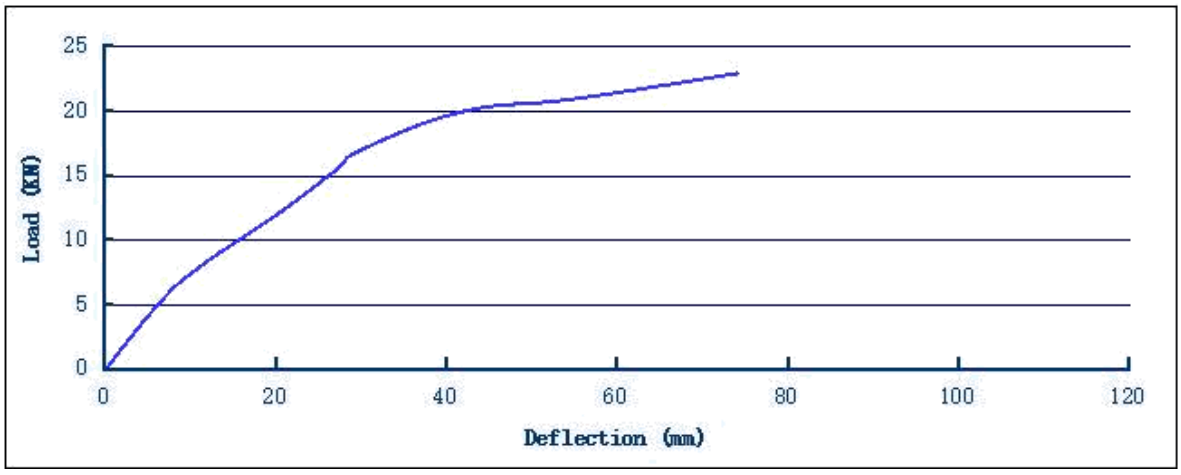

Fig 4.18 Load deflection of corroded beam after 7days at L/2 span

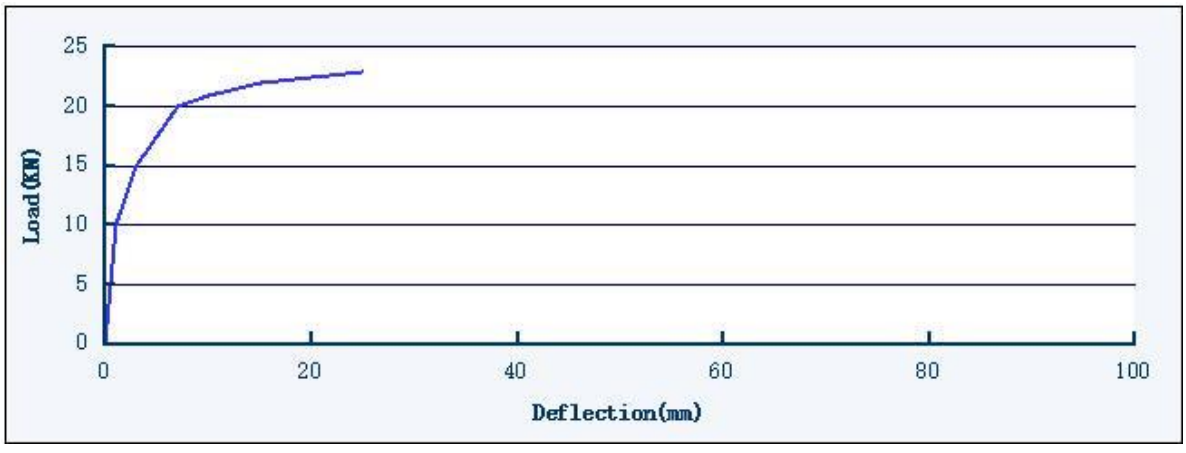

Fig 4.19 Load deflection curve for corroded beam after 7 days at L/4 span

4.2.3 Beams Corroded to 15-Days (C-15)

Beam undergoing corrosion for 15 days shows longitudinal crack throughout the corrosion region and some vertical cracks on side face before loading as shown in **Fig 4.20.**It was observed that first vertical crack appeared at a load of 16 KN near the centre of beam on side face, with widening of longitudinal crack at the centre and as the load on beam was increased, vertical crack from tension zone propagates towards the compression face till the longitudinal crack and finally beam fails at a load of 17.5 KN with a huge crack at centre of beam and further widening of the vertical crack and crushing of concrete from the extreme tensile face as shown in **Fig 4.21**.At ultimate load ultimate deflection noted at centre was 58 mm and at span/4 was 19.68 mm.**Table 4.3** shows load deflection behaviour and corresponding stiffness values at different points. It was observed from the curves shown in **Fig 4.22 and 4.23** that there is a decrease in load carrying capacity and deflection capacity of C-15 beam as compared to C-7 beam, control beam.

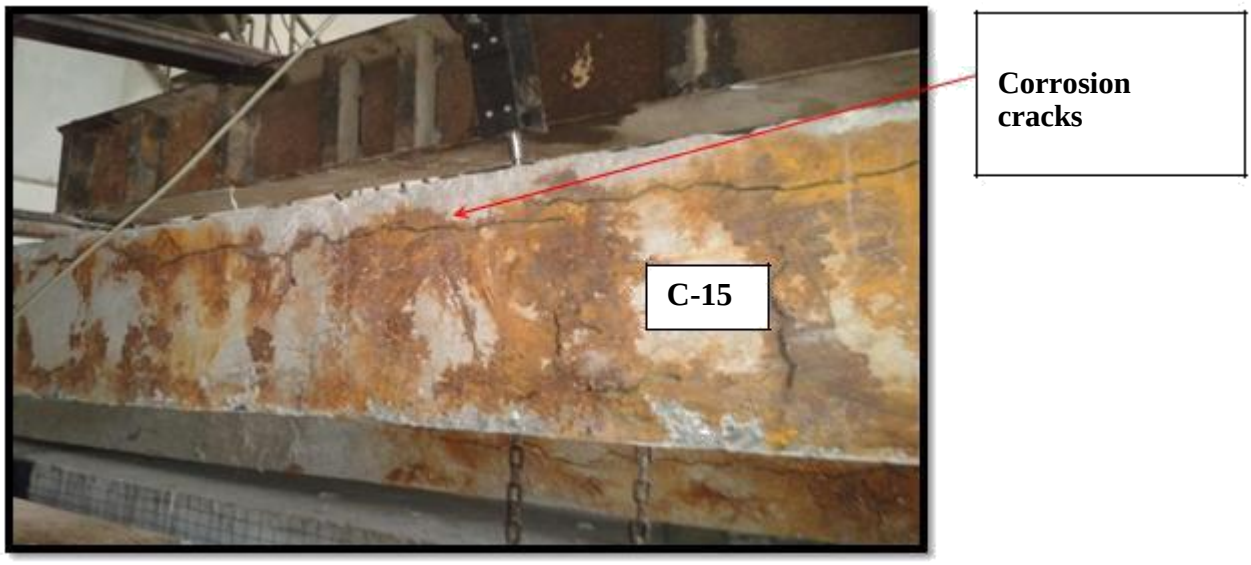

Fig 4.20 Side face of C-15 Beam before loading

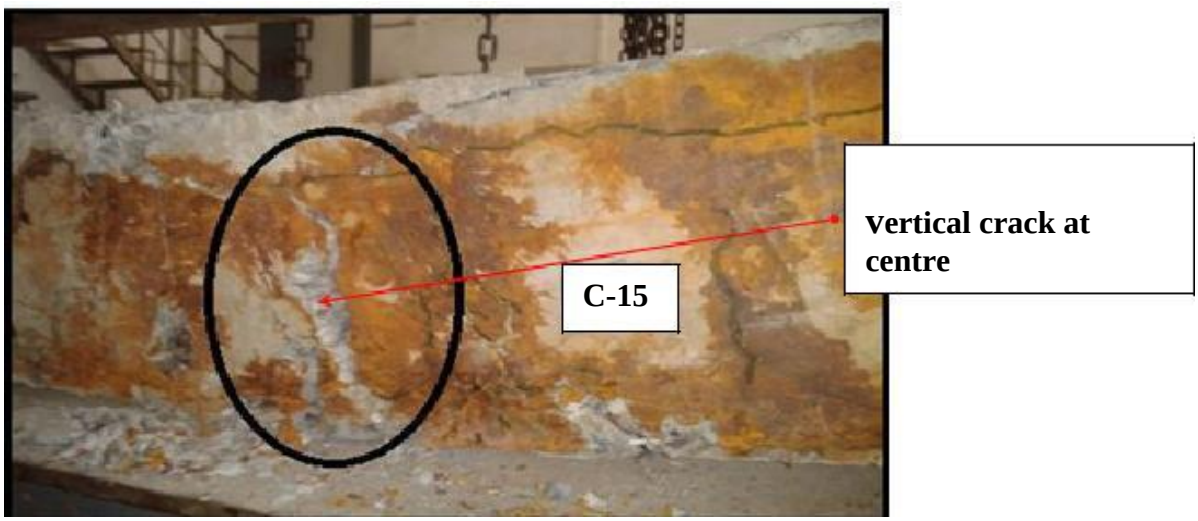

Fig 4.21 C-15 Beam showing large vertical crack near the centre of beam

Table 4.3 Load deflection values of beam subjected to 15 day corrosion

S.No.	Load (kN)	Deflection atL/2	
		Deflection (mm)	Stiffness (KN/mm)
1	0	0	0
2	5	8	0.625
3	8	14	0.57
4	13	23	0.56
5	14	30	0.46
6	15.5	35	0.44
7	16	38	0.42
8	17	45	0.37
9	17.5	58	0.301

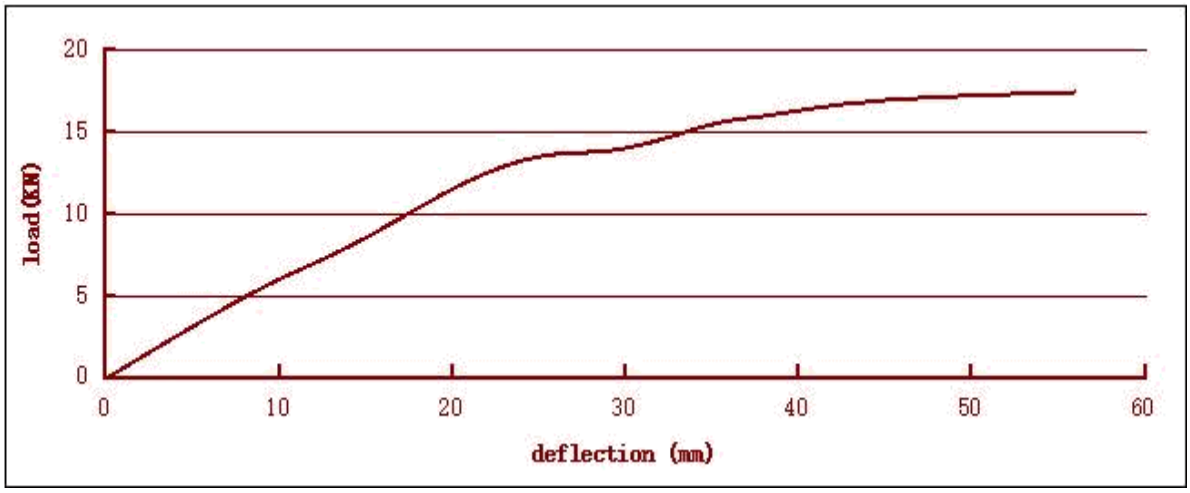

Fig 4.22 Load deflection characteristics of C-15 at L/2

Fig 4.23 Load deflection characteristics of C-15 at L/4

4.2.4 Beams corroded to 24 days (C-24)

Beam corroded to 24 days results in slightly breaking of beam at centre, it was totally damaged due to corrosion and was tested for load deflection characteristics. When the beam was tested under static loading it fails completely at 10 KN load with maximum deflection of 45 mm at centre.

4.3 Comparison of Load Deflection characteristices of all beam

After studying load deflection behaviour of all beams, it was concluded that it gives much information about the behviour of RC beams and how it changes with inducing corrosion in the beams.**Table 4.4** shows the stiffness loss in all beams when we compare the corroded beams with the control beam.As the corrrosion level increases we can correlate with the

visual inspection that cracks increases in beams leads to decrease in load carrying capacity of beams and hence stiffness decreases.**Fig 4.24** shows the graphical representation that how stiffness lost when corrosion level in beams increases

Table 4.4 Stiffness loss

Nomenclature	Ultimate load(kN)	Deflection L/2(mm)	Stiffness (KN/mm)	Stiffness loss (%)
C-0	26	80.08	0.32	0
C-7	23	74	0.31	3.10
C-15	17.5	56	0.30	6.25
C-24	10	45	0.22	31.25

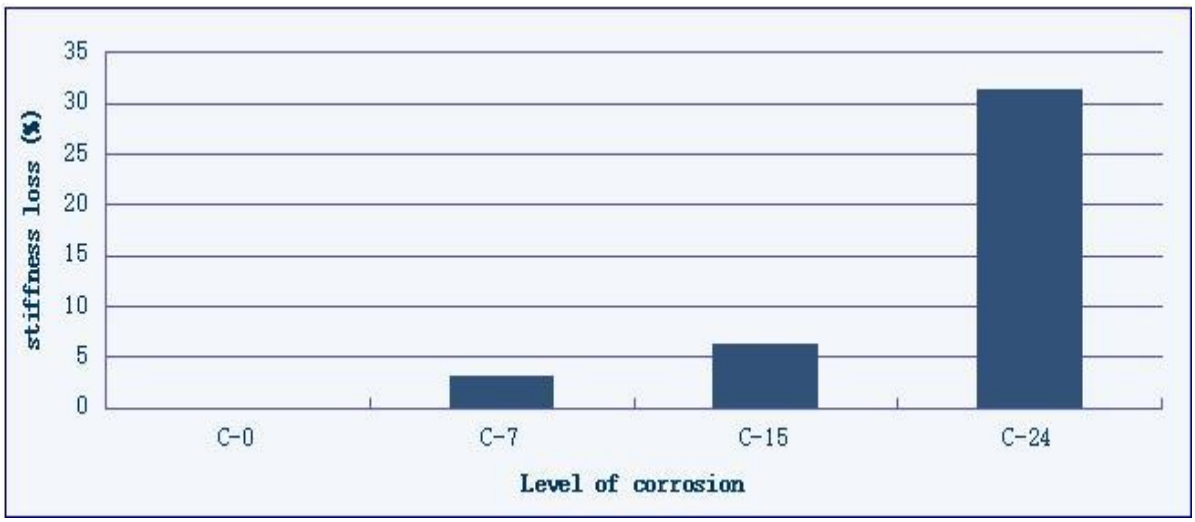

Fig 4.24 Bar chart showing stiffness loss with corosion in beam

Following results can be predicted from the above discussion that:-

- As the corrosion level increases , deflection at initial stages increases but leads to decrease in ultimate deflection of corroded beans than control .
- A higher corrosion level results in decreased stiffness
- Decrease in stiffness , load carrying capacity,deflection capacity suggests a change in behaviour of beams from ductile to brittle.

4.4 Vibration Characteristics of beams

In the experimental set up one beam is a control beam and other are corroded beams at different levels i.e 7 days,15 days,24 days .The vibration characteristics were studied on control beam and corroded beam and results were compared.In this study, changes in structural dynamic characteristics of control beam and damaged beams were investigated using the OROS software program with the help of impact hammer excitation test. One accelerometer was installed at center of beams to measure the response. The program was set up to make a measurement with a frequency range of 0 to 50 Hz.

To measure vibration response in this research, the first step is to set up an appropriate impulse-force hammer, transducer, and FFT analyzer. The mass and tip hardness of the hammer can be selected to give the desired magnitude and duration of the force pulse. Hammers can be constructed with weights ranging from a few grams up to several kilograms. They can cover a wide range of frequencies. In general, heavier hammers are more effective at lower frequencies. However, if the hammer is too heavy and the structure is too week, the hammer may overload the structure or rebound to cause a double hit. On the other hand, if the hammer is too light, there will not be enough energy imparted to the structure under test. The hammer tip also affects the impact. A steel tip will provide a short duration force with large amplitude. A rubber tip will provide a long duration force with small amplitude. A plastic tip falls somewhere between steel and rubber . In the frequency domain, a rubber tip will provide a narrow frequency response range, a steel tip will provide a wide frequency response range and a plastic tip again falls somewhere between the two. The testing object is also a consideration in tip selection because one does not want to permanently damage the structure under test. Impact hammers are supplied with calibration values for each hammer/tip combination. The proper tip can be selected based upon the desired frequency range and the mass of the structure under test.

Accelerometers are widely used transducers for dynamical property testing. The weight of a selected accelerometer is important because it may alter the dynamic characteristics of the structure under test. Dynamic mass loading is the change in physical properties of the structure caused by adding the mass of the accelerometer.

FRF measurement parameters can be set before taking measurement data, such as frequency range, number of signal lines, unit type, and so on.After applying each load step,

the dynamic characteristics rendered records in OROS based on a linear analysis setup. These records included trigger hammer plot, time history plot, and frequency response function plot, which gave the amplitude of vibration along with frequency.

Triggering: - Triggering is a technique for capturing an event for which it is not known exactly when it will occur. A trigger can start data acquisition and processing when a user specified voltage level is detected in and input channel. For example, we can set up a trigger to capture a hammer impact. After the trigger is armed, the analyzer will wait until the impact occurs before it starts acquiring data.

Frequency Response Function (FRF):- FRF is computed from two signals. It is sometimes called a "transfer function". The FRF describes the level of one signal relative to another signal. It is commonly used in modal analysis where the vibration response of the structure is measured relative to the force input of impact hammer or shaker. The estimation of FRF depends upon the transformation of data from time to frequency domain. The Fourier transform is used for this computation. Unfortunately, though, the integral Fourier transform definition requires time histories from negative to positive infinity. Since this is not possible experimentally the computation is performed digitally using a Fast Fourier Transform (FFT) algorithm which is based upon only a limited time history. In this way the theoretical advantages of the Fourier transform can be implemented in a digital computation scheme.

Fast Fourier Transform (FFT):- It is the discrete Fourier transform of a block of time signal. It represents the frequency spectrum of the time signal. It is a complex signal meaning that it has both magnitude and phase information

FRF is a useful tool because it relates to three major structural parameters: mass, damping, and stiffness. Although, it is difficult task to calculate FRF by using classical method but modal analysis always obtain structural mode shape from measured FRF. To avoid this complicating effect, many concerned researchers mention only the fundamental measured FRF because FRF in higher mode are sensitive (Kanwar et al., 2006). **So this section discusses the fundamental natural frequencies of all beams.**

4.4.1 Control beam (C-0)

The fundamental frequency of control beam (C-0) comes out to be 10 Hertz and the FRF magnitude was 0.52 g/N as shown in **Fig 4.25**. Value of analytical frequency comes out to be 12.87 hertz.Error in experimental and analytical values of frequency= $\frac{12.87-10}{12.87} = 0.222$

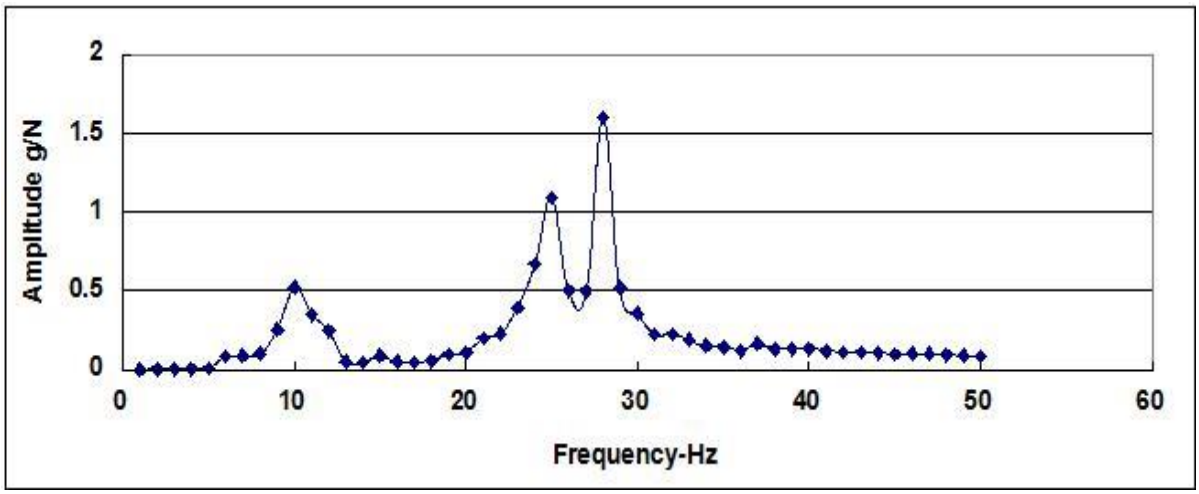

Fig 4.25 FRF record of control beam

4.4.2 Beam corroded to 7 days (C-7)

The fundamental frequency of corroded beam (C-7) comes out to be 9 Hertz and the FRF magnitude was 0.5 g/N as shown in **Fig 4.26.** As compared to control beam , frequency of corroded beam decreases from 10 to 9 hertz and so is the change in FRF magnitude, it also decreases as compared to control beam.

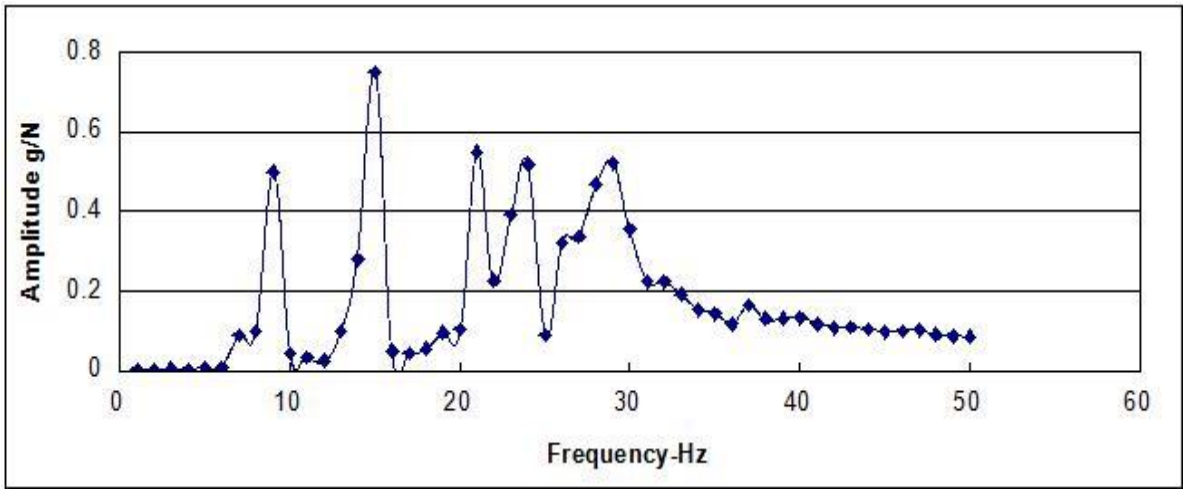

Fig 4.26 FRF record of corroded beam to 7 days

4.4.3 Beam corroded to 15 days(C-15)

The fundamental frequency of corroded beam (C-15) comes out to be 8 Hertz and the FRF magnitude was 0.257 g/N as shown in **Fig 4.27**. As the corrosion level increases from 7 days to 15 days there is more decrease in frequency and FRF magnitude as compared to control beam.

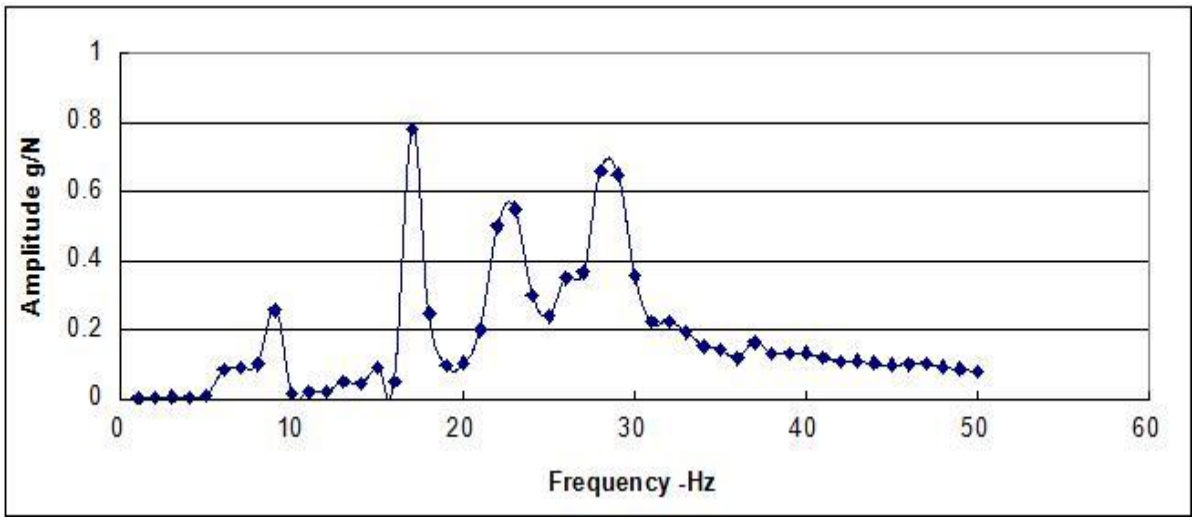

Fig 4.27 FRF record of corroded beam to 15 days

4.4.4 Beam corroded to 24 days(C-24)

The fundamental frequency of corroded beam (C-24) comes out to be 8 Hertz and the FRF magnitude was 0.25 g/N as shown in **Fig 4.28**. As the corrosion level increases from 15 days to 24 days there is not much change in frequency but FRF magnitude slightly decreases as compared to beam corroded to 15 days, but if compared with corroded beam there is notable decrease in frequency and FRF amplitude.

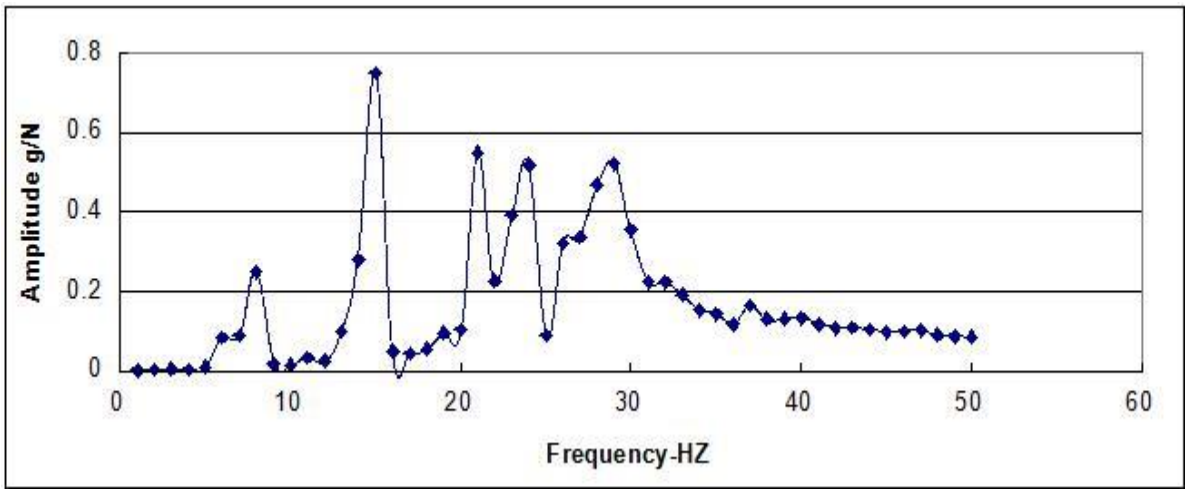

Fig 4.28 FRF record of corroded beam to 24 days

4.5 Variation in frequency with different levels of corrosion

After studying the FRF records of all beams,minor shift in the frequency was observed as the level of corrosion increases.

- There is decrease in natural frequency with increase in corrosion. As the corrosion level increases in the beams ,cracks increases in beams results in decrease in frequency as compared to control beam
- It corroborates well with the increasing damage as observed in visual inspection with increase in corrosion.
- Similarly as the level of corrosion increases, load at failure reduces pointing towards stiffness loss with increase in corrosion
- In the same way as shown in **Table 4.5** natural frequency falls due to huge degradation of beam due to corrosion.However at higher level of corrosion there is no significant decrease in frequency but its change in comparison of control beam is notable

Table 4.5 Variation of frequency with level of corrosion

Sr No.	Nomenclature	Frequency (Hertz)
1	C-0	10
2	C-7	9
3	C-15	8
4	C-24	8

Fig 4.29 shows graphically the variation of frequency with different levels of corrosion

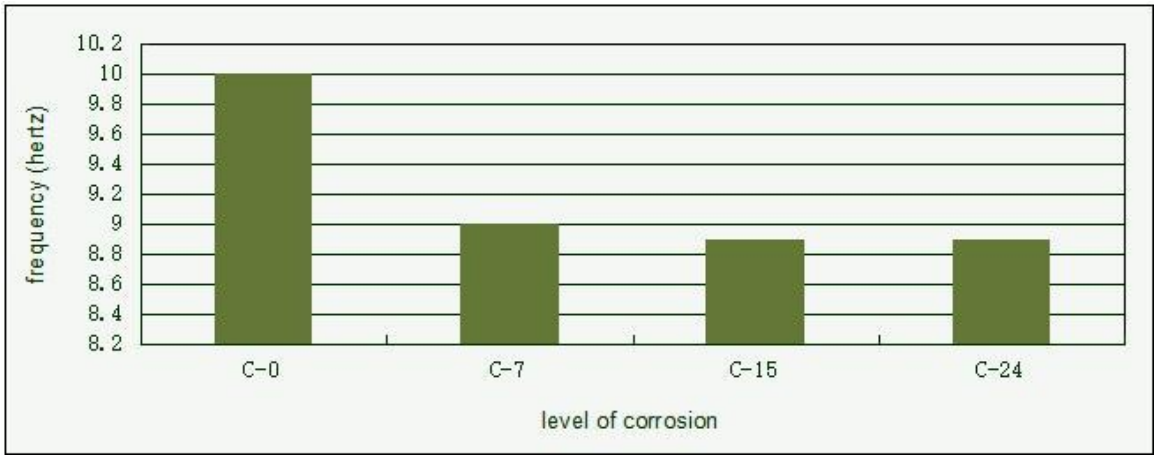

Fig 4.29 Bar chart showing relation between level of corrosion with frequency

4.6 Variation of FRF amplitude with different levels of corrosion

After studying the FRF records of all beams,minor shift in the FRF amplitude was observed as the level of corrosion increases.

- FRF magnitude showed a huge decrease with increase in corrosion. As the corrosion level increases in the beams ,cracks increases in beams results in decrease in FRF magnitude as compared to control beam
- It corroborates well with the increasing damage as observed in visual inspection with increase in corrosion.
- Similarly as the level of corrosion increases, load at failure reduces pointing towards stiffness loss with increase in corrosion
- In the same way as shown in **Table 4.6** FRF amplitude decreases due to huge degradation of beam due to corrosion

Table 4.6 Variation of FRF amplitude with different levels of corrosion

Sr No.	Nomenclature	FRF amplitude (m g/N)
1	C-0	0.52
2	C-7	0.50
3	C-15	0.257
4	C-24	0.25

From **Fig 4.30** it is clearly seen that as we increase the level of corrosion ,it results in decrease in FRF amplitude as compared to control beam.

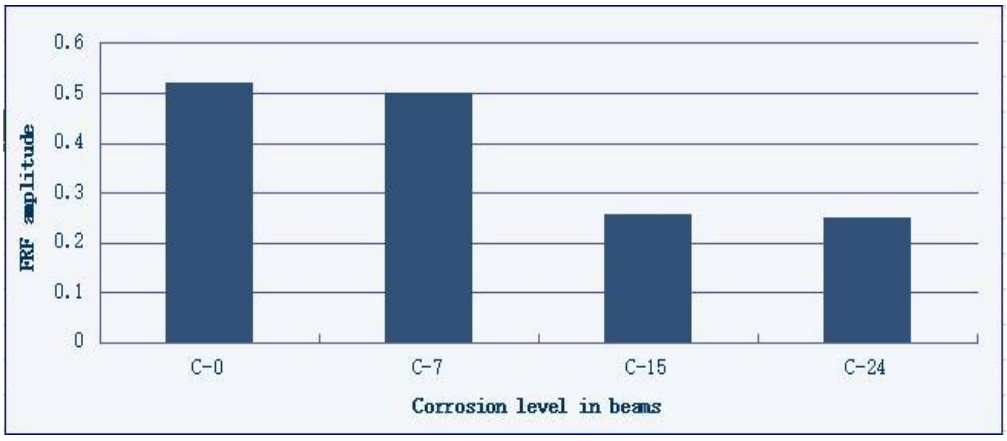

Fig 4.30 Bar chart showing relation between level of corrosion with FRF amplitude

4.7 Calculations of Damage Index

Damage index is a measure of damage due to corrosion in beams.Damage Index is defined as change in stiffness to the original stiffness depicted static characteristices of beam and well matches with dynamic characteristices of beams i.e natural frequency and FRF magnitude decreases with increase in damage due to corrrosion. **Table 4.7** shows variation of damage index with FRF magnitude and frequency.**Fig 4.31** shows graphically that with increase in damage index FRF magnitude decreases

Table 4 .7 Variation of damage index with FRF magnitude and frequency

Sr No.	Nomenclature	FRF magnitude (m g/N)	Frequency (Hz)	Damage index
1	Beam	0.52	10	0
2	C-7	0.5	9	0.031
3	C-15	0.257	8	0.059
4	C-24	0.25	8	.3125

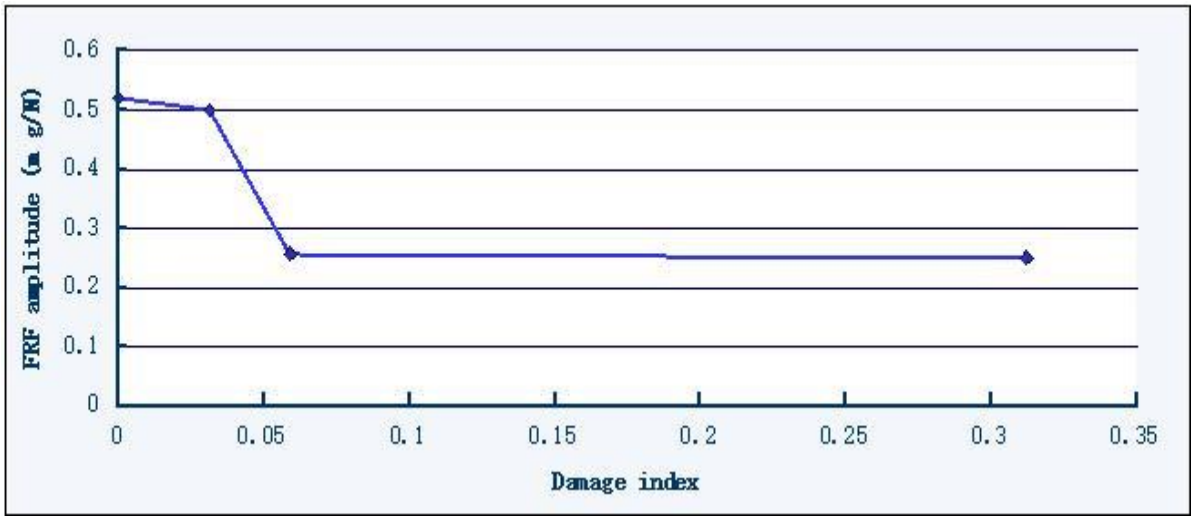

Fig 4.31 Graph showing relation between damage index and FRF magnitude

4.8 Closing Remarks

This chapter highlights the results obtained from the experiments done during the thesis work. It shows results of visual observations of RC beams subjected to different levels of corrosion and its effect on load deflection behavior when the RC beams were tested under static four point loading. From the results it was observed that there is decrease in ultimate load, deflection capacity, stiffness as the corrosion level increases.This section also deals with the results of FRF recorded during vibration monitoring of RC beam which shows the effect of corrosion on dynamic properties of beams like natural frequency and FRF amplitude.

CHAPTER -5

CONCLUSIONS

5.1 VISUAL INSPECTION

From the reinforced concrete beams subjected to accelerated corrosion at different levels i.e.7 days, 15 days, 24days all beams were visually inspected and it was observed that as exposure time of the beams to corrosion increases deterioration increases. Following results are observed:

- For C-7 Beam shows only reddish brown corrosion patches on the centre 1.5 m portion of beam which was intentionally corroded and which act as a cathode. No cracks were developed on the surface of the beam
- For C-15 beam small horizontal and vertical cracks were seen on the surface of beam of increased length and width and increase in volume of corrosion product was noticed.

  Flexural crack also observed at centre of beam, corrosion liquid of reddish brown colour was seen oozing out from the cracks.
- For C-24 beams, it was observed that the cracks has covered full longitudinal length at middle 1.5m portion of RC beam and corrosion products generated were of dark

  reddish brown colour of increased volume that other beam with lot of corrosion liquid oozes out from the cracks.

This reddish brown product is a results of rusting of reinforcement in the beams and crack generation is because of tensile stresses generated due to increased volume of bar at cathode area, as we all know concrete is weak in tension so it results in cracking.concrete spalling is also observed during corrosion process.

5.2 STATIC ANALYSIS

Beams were subjected to static four point loading and load deflection curves reveal much information about the behaviour of beams and they are alterd with the effect of corrosion.static load tests showed the following results

- As the corrosion level increases , deflection at initial stages increases but leads to decrease in ultimate deflection of corroded beans than control .
- A higher corrosion level results in decreased stiffness

- Decrease in stiffness , load carrying capacity,deflection capacity suggests a change in behaviour of beams from ductile to brittle.

5.3 DYNAMIC ANALYSIS

Vibration analysis of beams was conducted using OROS software which gives us the FRF response of beams including maximum amplitude and frequency of control beam and corroded beams.

- As the level of corrosion increases from control beam to 7 days ,15 days, 24 days amplitude of vibrations goes on decreasing due to increased amount of deterioration
- Natural frequency of beam also decreases from 10Hz to 8 Hz with increasing level of corrosion
- With increasing damage index amplitude of vibrations decreases.

As observed by visual inspection , with increases in corrosion level, cracks developed in beams which effects the static as well as dynamic properties of beams.As the level of corrosion increases, load at failure reduces pointing towards stiffness loss with increase in corrosion . In the same manner there is a huge decrease in FRF amplitude and natural frequency due to increased deterioration of beams .

REFERENCES

- Andrade. C., Alonso, M. C. and Gonzalez. J. A.(1990**). An initial effort to use the corrosion rate measurements for estimating rebar durability.** 7, pp29–37.

- Almusallam, A. A., Al- Gahtani, A. S., Abdur Rauf Aziz and Rasheeduz zafar. (1996).**Effect of reinforcement corrosion on bond strength**. Construction and building materials,10, pp123–131.

- Acosta et al. (2004) **Influence of corrosion on structural stiffness of beams**,5,pp 1-15

- Andrade, C. Garcés, P. and Martínez, I. (2008). **Galvanic currents and corrosion rates of reinforce ments me asured in cells simulating different pitting areas caused by chloride attack in sodium hydroxide** . Corrosion Science 29,pp 59-64

- Burgueno, R., Karbhari, V. M., Seible F. and Kolozs, R. T. (2001). **Experimental Dynamic Characterization of an FRP composite Bridge Superstructure Assembly, Composite Structures**

- Baghiee N., Esfahani M. R. and Moslem K. (2009). **Studies on Damage and FRP Strengthening of Reinforced Concrete Beams by Vibration Monitoring, Engineering Structures,** 31,pp 875-893,427-444

- Broomfield, J. P. (1997 **). Corrosion of steel in concrete: understanding, investigation, and repair,** E&FN Spon, London.

- Dionysius, M. Siringoringo, Yozo , Fujino (2005). **Experimental study of laser Doppler vibrometer and ambient vibration for vibration-based damage detection, Journal of structural engineering,**28, pp 1803-1815

- Joyce, T. A. (2008). **The Effects of Steel Reinforcement Corrosion on The Flexural Capacity and Stiffness of Reinforced Concrete Beams** . MASc Thesis, Ryerson University, Toronto

- Jeong et al.(2005) **Vibration based monitoring in model plate girder bridges**

- Kanwar, V., Kwatra, N., Aggarwal, P. and Gambir, M.L. (2006). **Vibration Monitoring of a RCC Building Model,** *Proceedings of National Conference on Technology for Disaster Mitigation*, Hamirpur, India.

- Kim,J.T., Park J.H. and Lee.B.H. (2005). **Vibration-based damage monitoring in model plate-girder bridges under uncertain temperature conditions**, Journal of structural engineering,15,pp 1300-1521

- Kessler, S. S., Spearing, S. M., Attala, M. J., Cesnik, C. E. S. and Soutis, C. (2002)**Damage Detection in Composite Materials Using Frequency Response Methods ,**33, pp 87-95.

- Maaddaway E.I. , Soudki K. (2003). **Effectiveness of impressed current technique to simulate corrosion of steel reinforce ment in concrete** ,15,pp 41-71.

- Maeck, J. (2003). **Damage assessment of Civil Engineering Structures by Vibration Monitori**ng, Ph.D. Thesis. Department of Civil Engineering, K. U. Leuven, Belgium.

- Maia, N.M.M., Silva, J.M.M., Almas, E.A.M. and Sampaio, R.P.C. (2002). **Damage Detection in Structures: from Mode Shape to Frequency Response Function Methods**, *Mechanical Systems and Signal Processing*, **17**(3): 489-498.

- Malumbela,G. , Mark,A. and Moyo.P. (2009). **Steel corrosion on RC structures under sustained service loads -A critical review.** Department of Civil Eng., University of Cape Town, Private Bag X3, Rondebosch, 7700, South Africa,14,pp 1720-1810

- Ndambi, J. M., Vantomme, J. and Devisscher, J. (2000). **Modal Damping as A Damage Detection Parameter in Reinforced Concrete structures,** Proceedings of the 5th international Conference on Computational Structures Technology, Leuven, pp. 1-7.

- Rao, J. S. (2000). **Vibratory Condition Monitoring of Machines,** Narosa Publishing House, New Delhi, India pp 1-4

- Smith, Roger W., (2007). **The effects of corrosion on the performance of reinforced concrete beams** . Master Thesis. Toronto, Canada,12, pp 149-162

- Song , H. W. ,Saraswathy, V. , (2006) **. Non destructive techniques to monitor corrosion .**

- Thalapil. j , Maiti. S. K. (2014)**Natural vibrations of monolithi cal beams with longitudnal cracks .**

- Vimuttasoongviriya, A., Kwatra, N. and Kumar, M. (2011) **Vibration monitoring of retrofitted RC beams using GFRP,**Phd Thesis, Thapar university, Patiala,India.

- Waters, M.J. Brennan, S. Sasananan (2003). **Identifying the foundation stiffness of a partially embedded post from vibration measurements**, Journal of Sound and Vibration, Vol. No.274, pp. 137–161

- Webster, M, P., (2000). **The Assessment of Corrosion damaged concrete structures.** A Thesis submitted to The University of Birmingham for the degree of Doctor of Philosophy.

- Wang, L., Li, C., and Yi, J., (2015). **An experiment study on behavior of corrosion RC beams with different concrete strength.** Recent Developments on Port and Ocean Engineering. Journal of Coastal Research, 73, pp.259-264.

- Yao, G.C., Chang, K.C. and Lee, G.C. (1992). **Damage diagnosis of steel frames using vibrational signature analysis,** Journal of engineering mechanic, ASCE,118, No. 9, pp. 1949-1961.

- Yong, X., Hong,H., Zanardob,G. and Deeksa,A.(2006). **Long term vibration monitoring of an RC slab: Temperature and humidity effect,** Journal of structural engineering , 28,pp. 441–452